Joint Institute for Nuclear Research
Dzhelepov Laboratory of Nuclear Problems

13th APCTP – BLTP JINR Joint Workshop
"Modern Problems in Nuclear and Elementary Particle Physics"

Ordinary muon capture studies by means of γ-spectroscopy

D. Zinatulina, V. Egorov, V, Brudanin, S. Kazarcev, N. Rumyantseva,

M. Shirchenko, E. Shevchik, I. Zhitnikov

16/07/2019, Dubna

Ordinary Muon Capture (OMC)

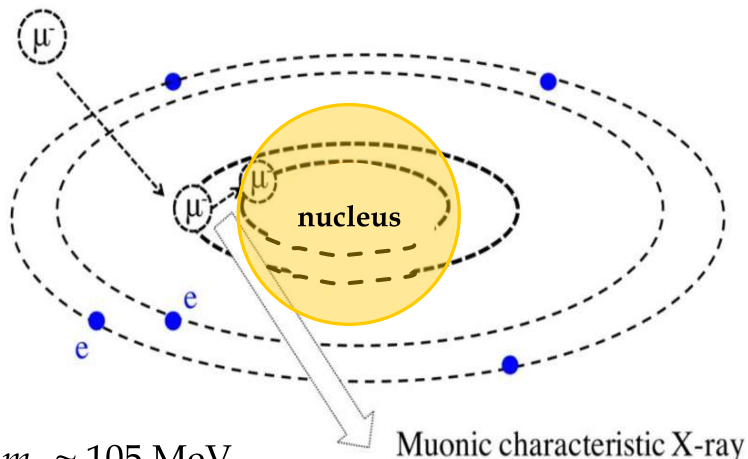

$m_{\mu} \sim 105$ MeV

$\mu^- \rightarrow e^- + \nu_e + \nu_\mu$ $\quad \tau_{dec} = 2.2\mu s$

$(A, Z) + \mu^- \rightarrow (A, Z\text{-}1)^* + \nu_\mu$

$\rightarrow (A, Z\text{-}1) + \gamma$

$\rightarrow (A\text{-}1, Z\text{-}1) + \gamma + n$

$\rightarrow (A\text{-}2, Z\text{-}1) + \gamma + 2n$

$\rightarrow (A\text{-}1, Z\text{-}2) + \gamma + n + p$

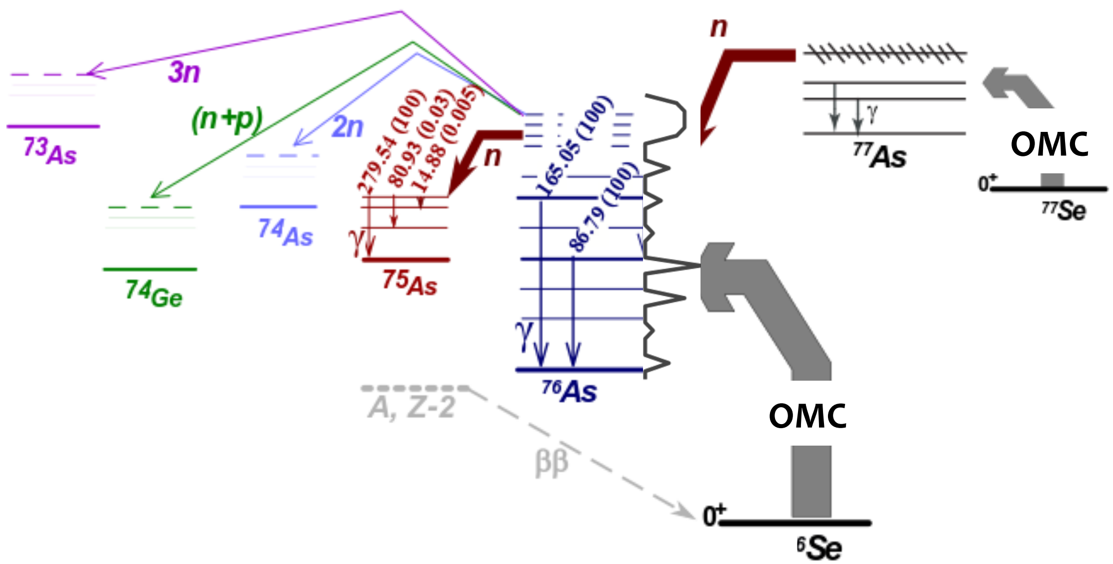

- Muonic cascades (our by-product)
- High momentum transfer (up to 100 MeV) -- High-lying states population
- **Right leg testing for DBD calculations (coupling to charge exchange reactions)**
- g_a – suppression probing -- via capture rates calculations (+ other methods)
- Angular correlations in OMC (Doppler shape of γ-lines)

Experimental input for NME calculations

$$\frac{1}{T_{1/2}^{0\nu}} \propto \left|\sum_i U_{ei}^2 m_i\right|^2 G^{0\nu} \left|\langle A,Z+2|S|A,Z\rangle\right|^2$$

$$\langle m_{\beta\beta}\rangle \qquad M^{0\nu}$$

$$\langle A,Z+2|S|A,Z\rangle \propto \sum_n \langle Z+2|\hat{H}|Z+1,n\rangle\langle Z+1,n|\hat{H}|Z\rangle$$

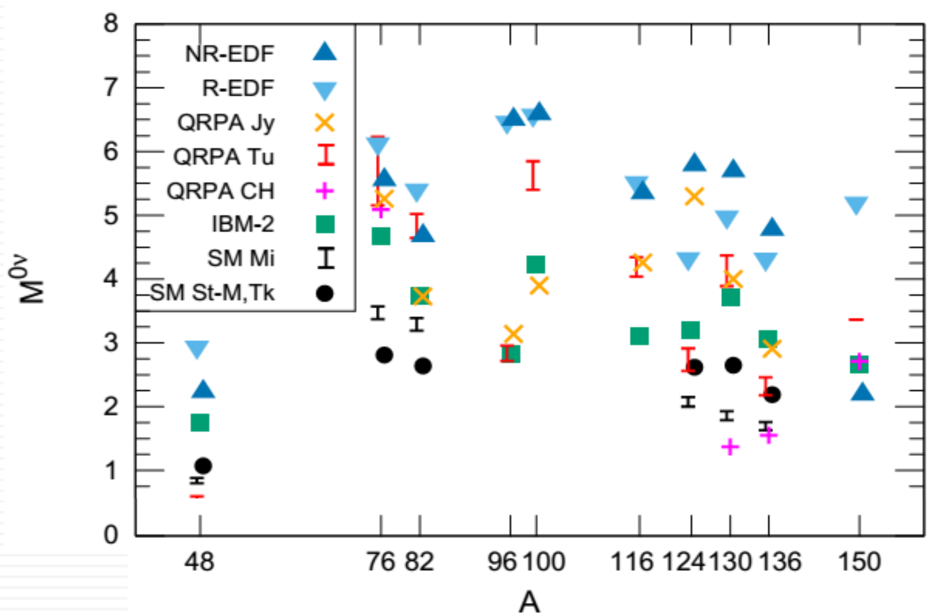

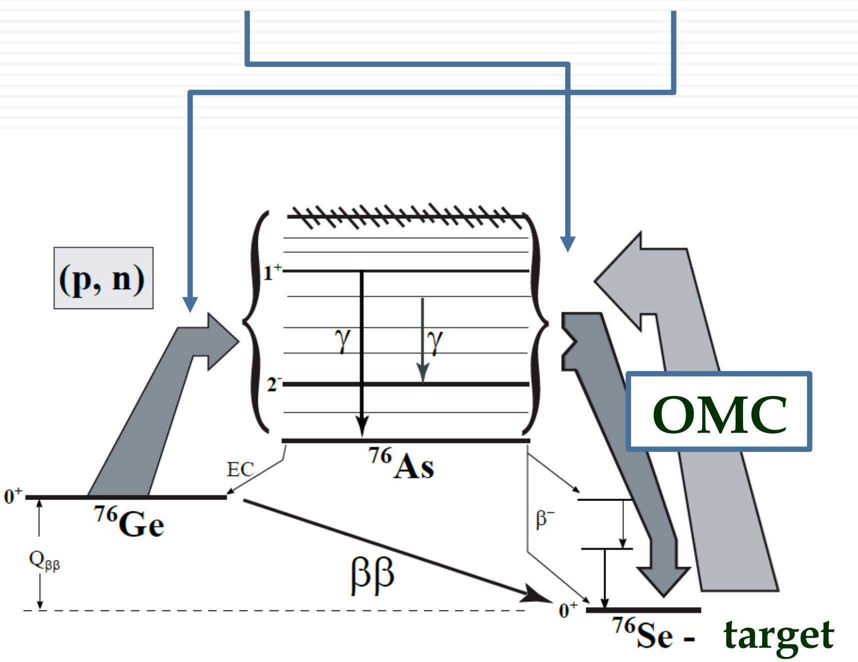

Measurement set-up

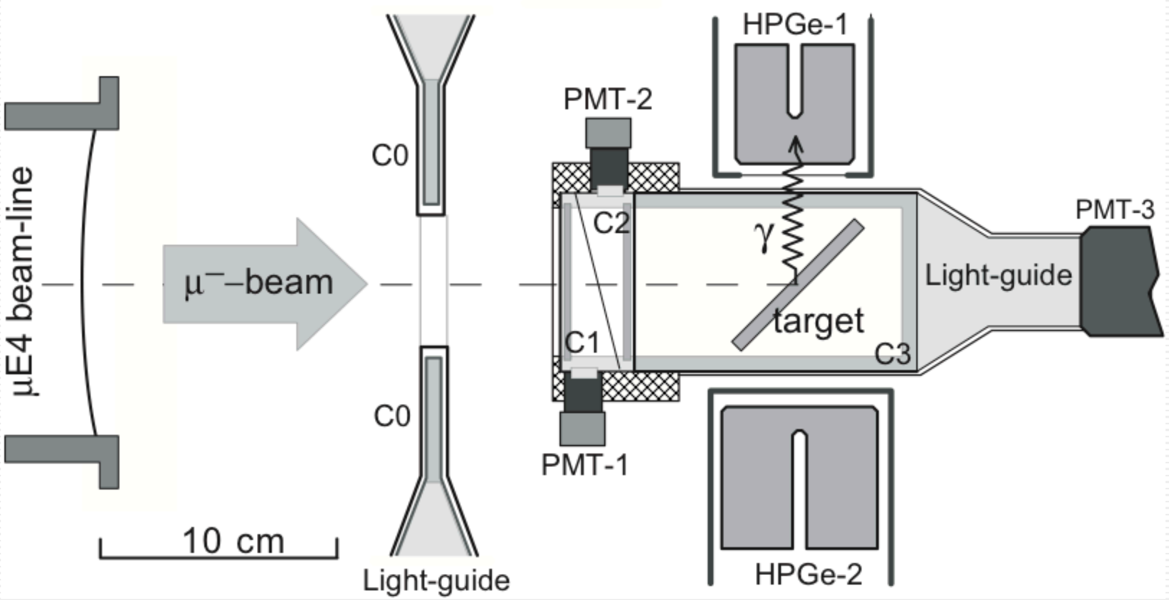

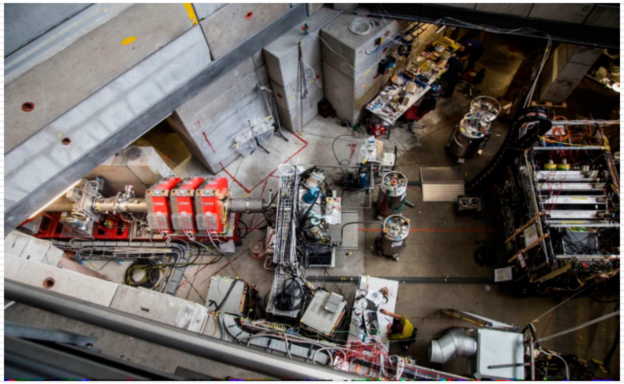

$$\mu_{stop} = \overline{C0} \wedge C1 \wedge C2 \wedge \overline{C3}$$

Number of μ-stop = (8 – 25) x 10³ with 20 – 30 MeV/c

HPGe's: register μX- and γ-radiation, following OMC in the target, and time

2β-decay	2β-experiments	OMC target	Status
^{76}Ge	GerdaI/II, Majorana Demonstrator	^{76}Se	2004 (PSI)
^{48}Ca	TGV, NEMO3, Candles III	^{48}Ti	2002 (PSI)
^{106}Cd	TGV	^{106}Cd	2004 (PSI)
^{82}Se	NEMO3, SuperNEMO, Lucifer(R&D)	^{82}Kr	2006 (PSI)
^{100}Mo	NEMO3, AMoRE(R&D), LUMINEU(R&D)	^{100}Ru	2018 (RCNP)
^{116}Cd	NEMO3, Cobra	^{116}Sn	2002
^{150}Nd	SuperNEMO, DCBA(R&D)	^{150}Sm	2006 (PSI)
^{136}Xe	EXO200, Kamland-Zen, NEXT	^{136}Ba	2019 (RCNP)
^{130}Te	Cuore 0/Cuore, SNO+	^{130}Xe	2019 (PSI)

(E, t) distribution of the correlated events following μ-capture in ^{76}Se target

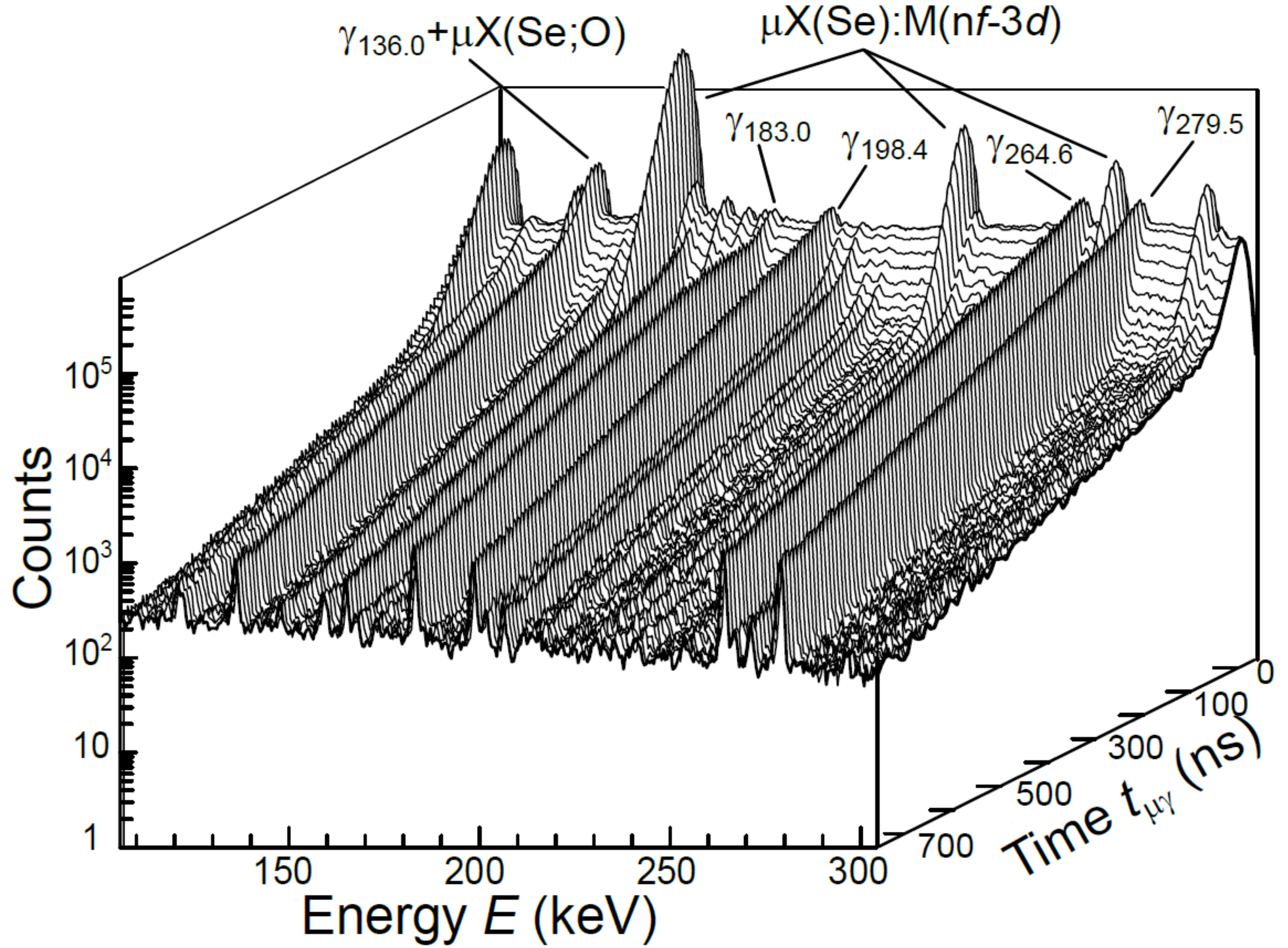

(*E*, *t*) distribution of the correlated events following μ-capture in ^{76}Se target

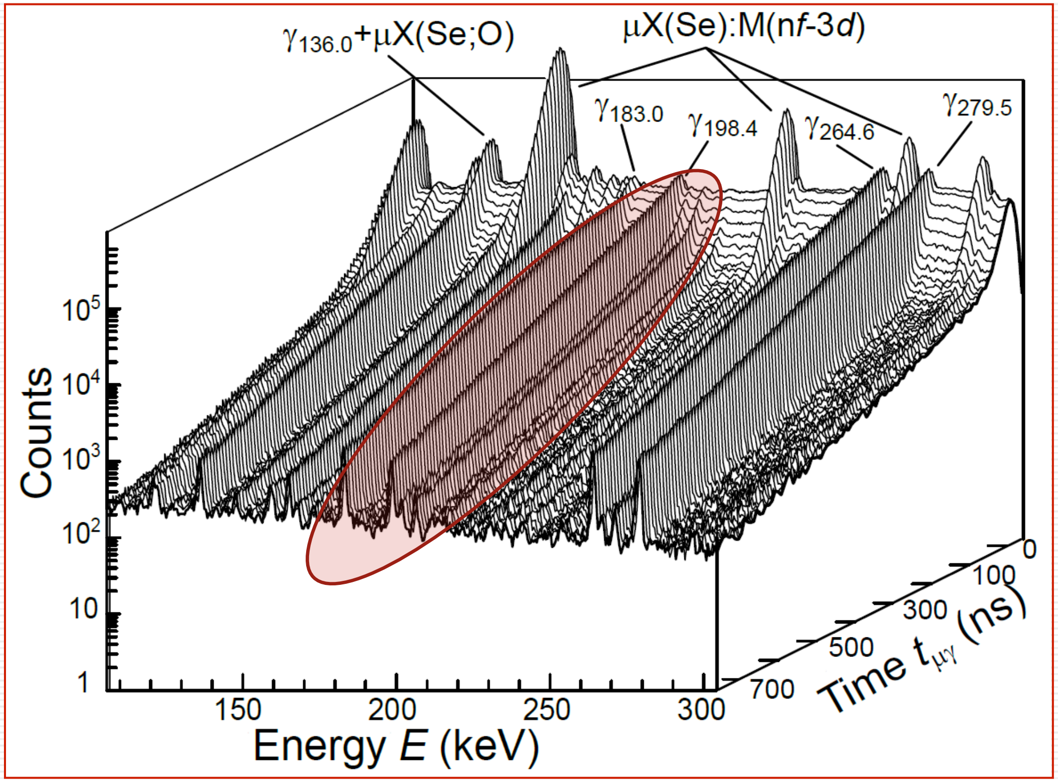

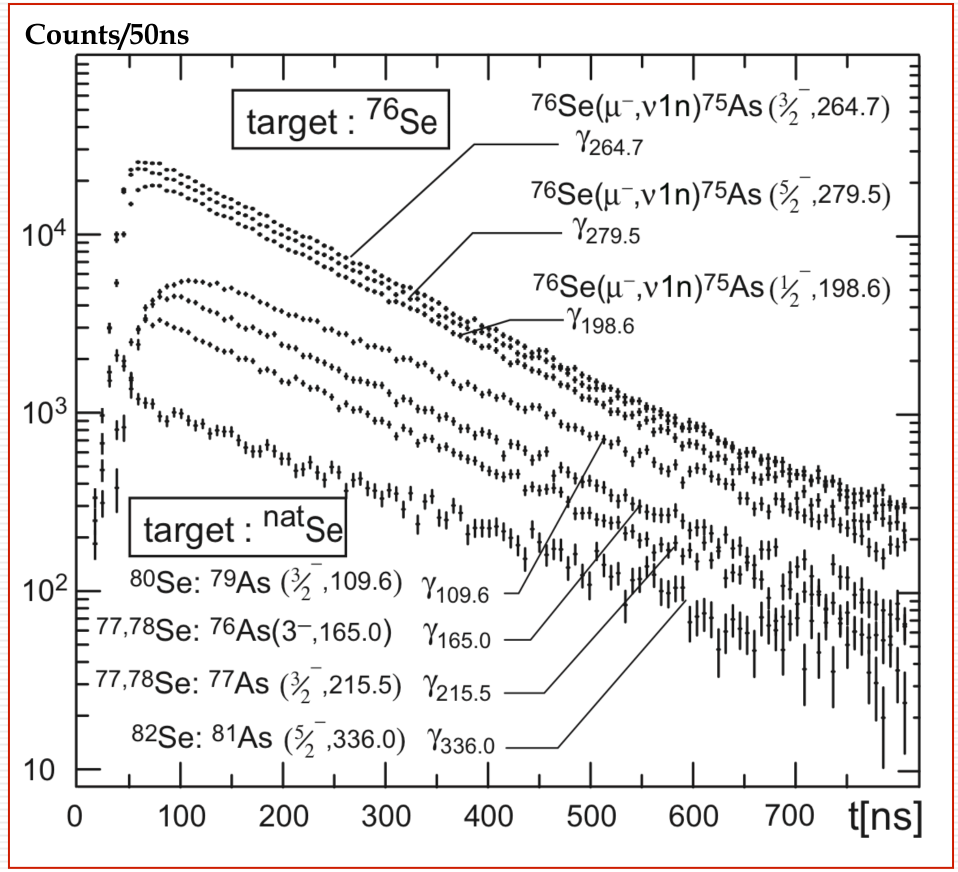

Time evolution of the intensities of the strongest γ-lines following OMC in ^{76}Se (top) и ^{nat}Se (bottom).

Total μ-capture rates in different isotopes of Se

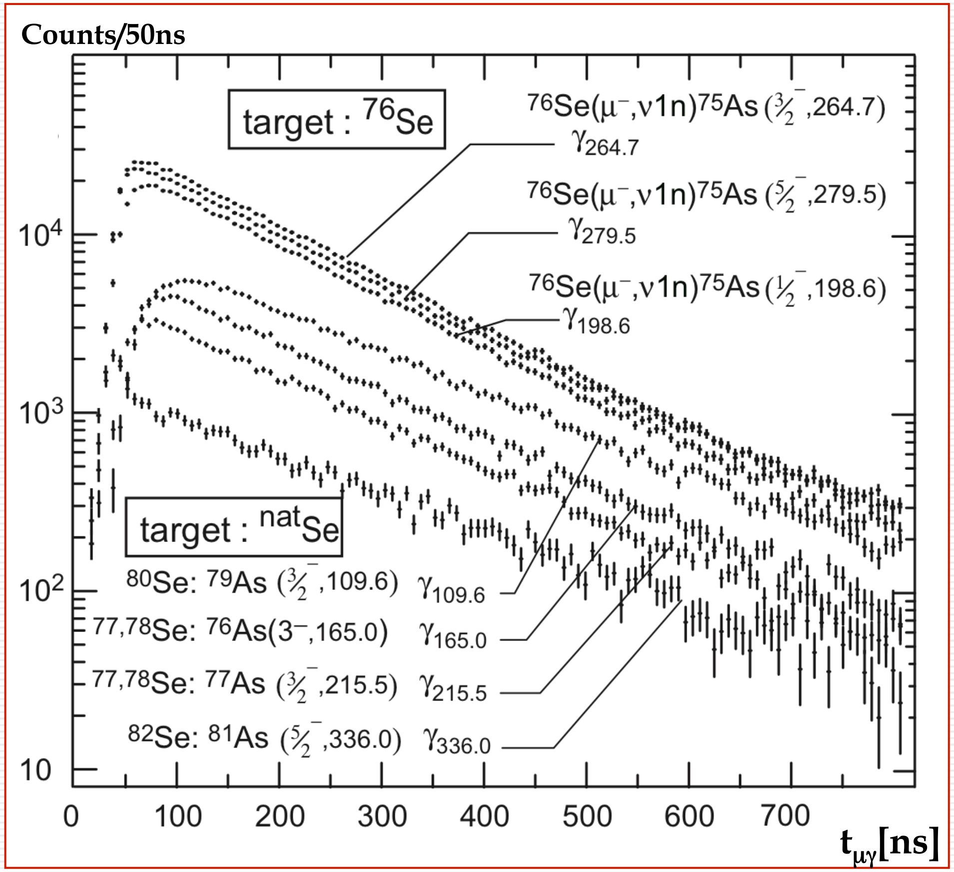

Time evolution of the intensities of the strongest γ-lines following OMC in ^{76}Se (top) и ^{nat}Se (bottom) [A].

Target	Daugh. Nuclei	E_i^γ [keV]	τ [ns]	$\langle\lambda_{cap}\rangle$ [10^6 c^{-1}]
^{76}Se [A]	^{75}As	198.6	148.4(7)	
		279.5	148.6(5)	
			<148.48(10)>	**6.300(4)**
^{nat}Se [A]				
$^{(77)}$Se	^{76}As	164.7	**163.5(20)**	**5.68(7)**
$^{(78)}$Se	^{77}As	215.5	**165.9(19)**	**5.59(7)**
$^{(80)}$Se	^{79}As	109.7	**185.5(27)**	**4.96(7)**
$^{(82)}$Se	^{81}As	336.0	**208.2(68)**	**4.37(14)**
^{nat}Se [B]			**163.5(10)**	**5.681(37)**

[A] D. Zinatulina, V. Egorov et al. // Phys. Rev. C 99(2019)024327

[B] T. Suzuki, D.F. Measday // Phys. Rev. C 35(1987)2212

Energy spectra in OMC

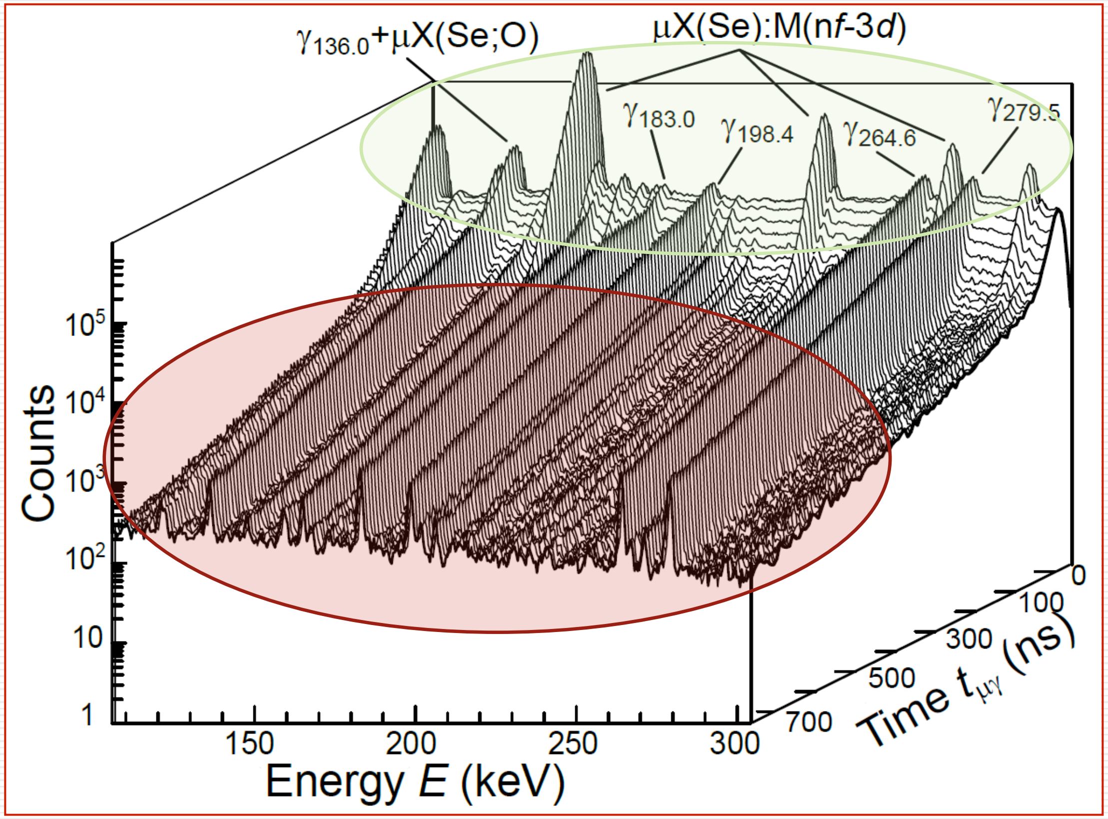

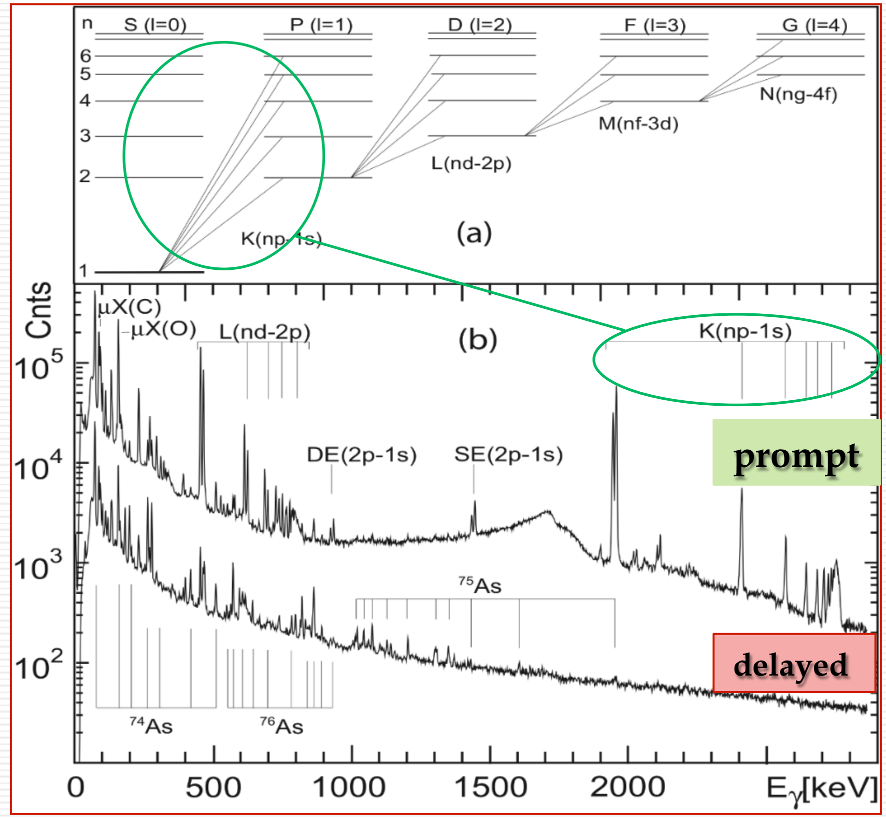

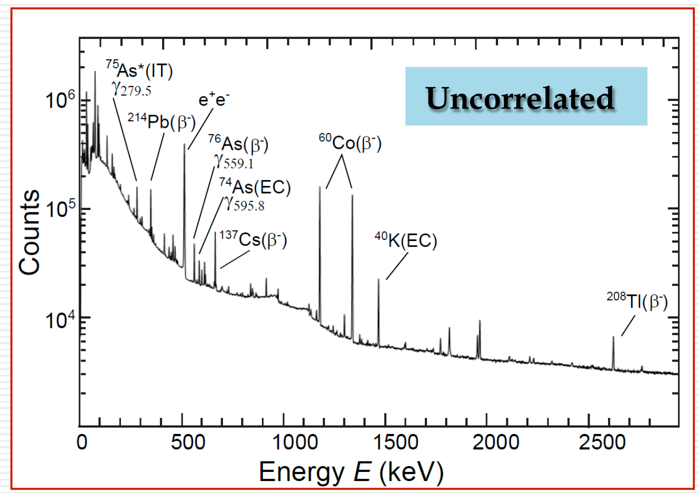

Energy spectra in OMC

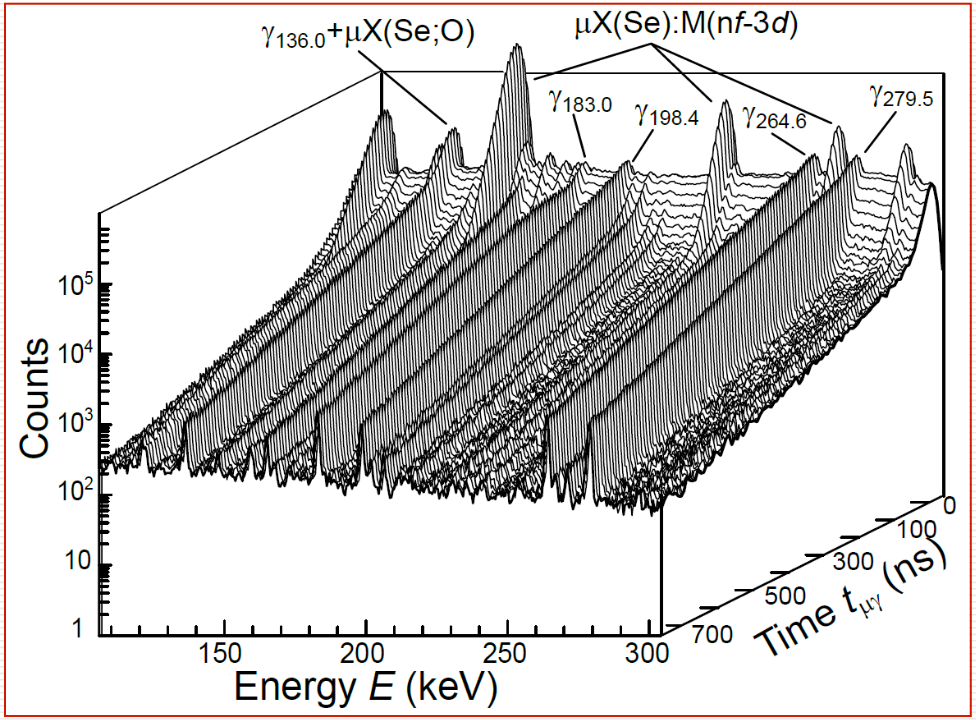

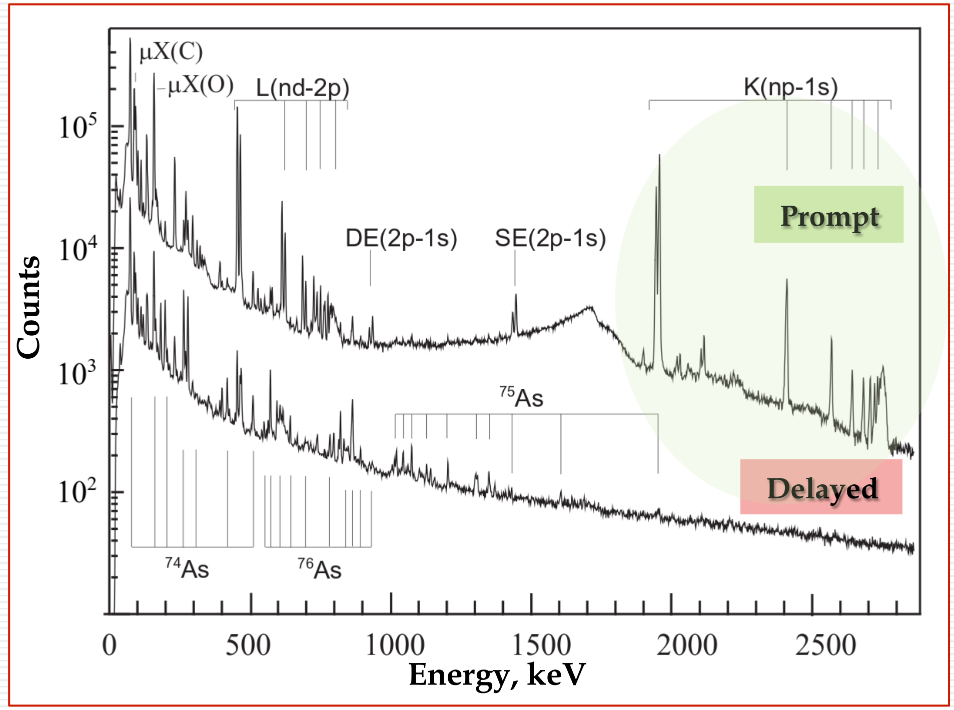

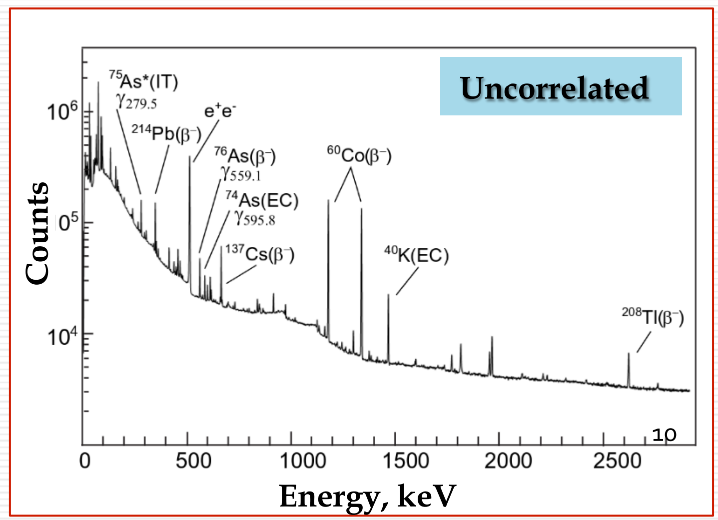

- $t_{\mu\gamma}$ = 0-50 ns: μX-cascades (**Prompt** spectra) – normalization, identification, composition of the surrounded materials and target itself;
- $t_{\mu\gamma}$ = 50-700 ns: γ-radiation following OMC (**Delayed** spectra) – partial μ-capture rates – strength function of the right side;
- T >> $t_{\mu\gamma}$: background radiation (**Uncorrelated** spectra) – calibration of the det-s, identification, yields of short-lived RI during exposure

Partial μ-capture probabilities to ^{76}As

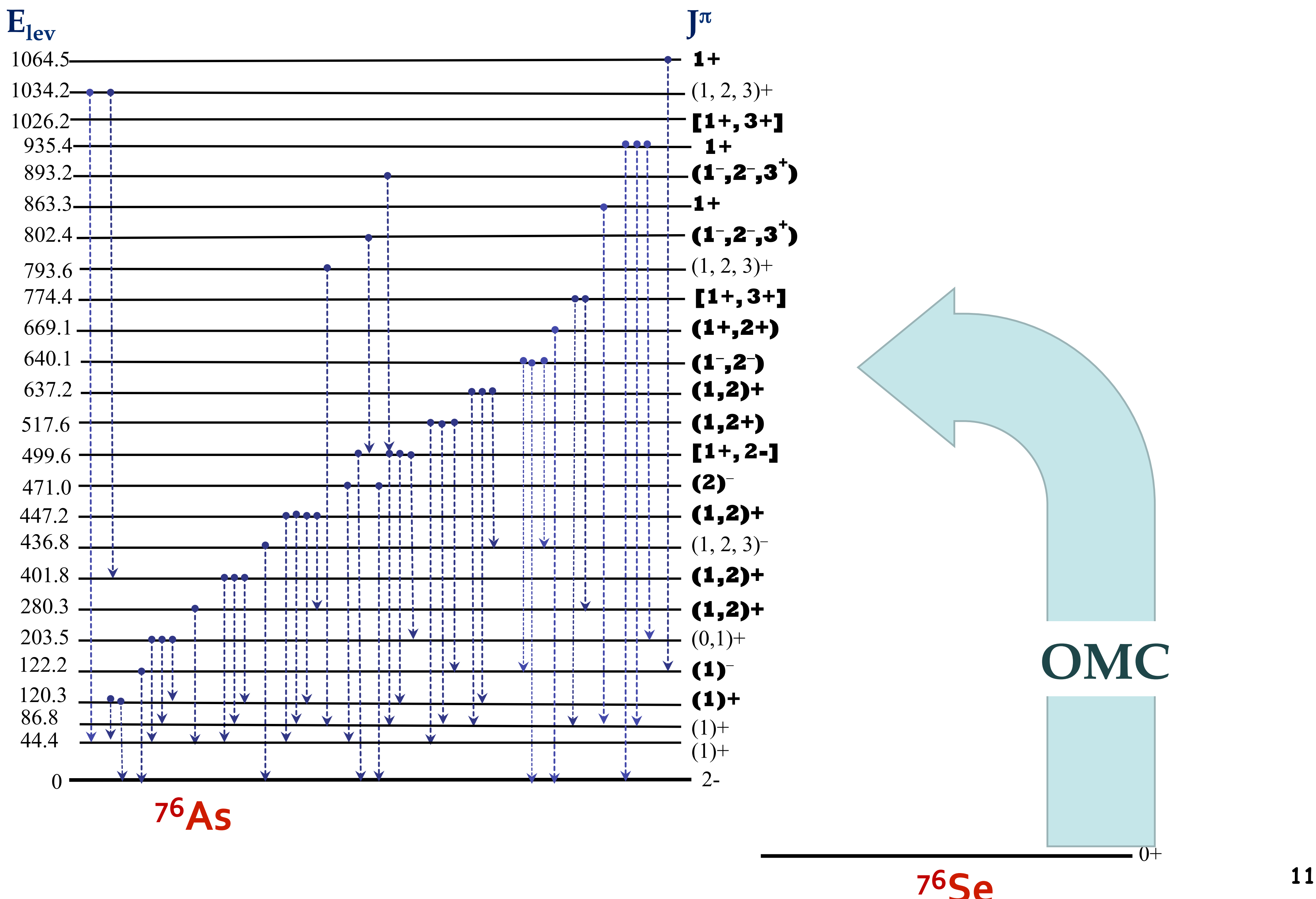

Partial μ-capture probabilities to ^{76}As

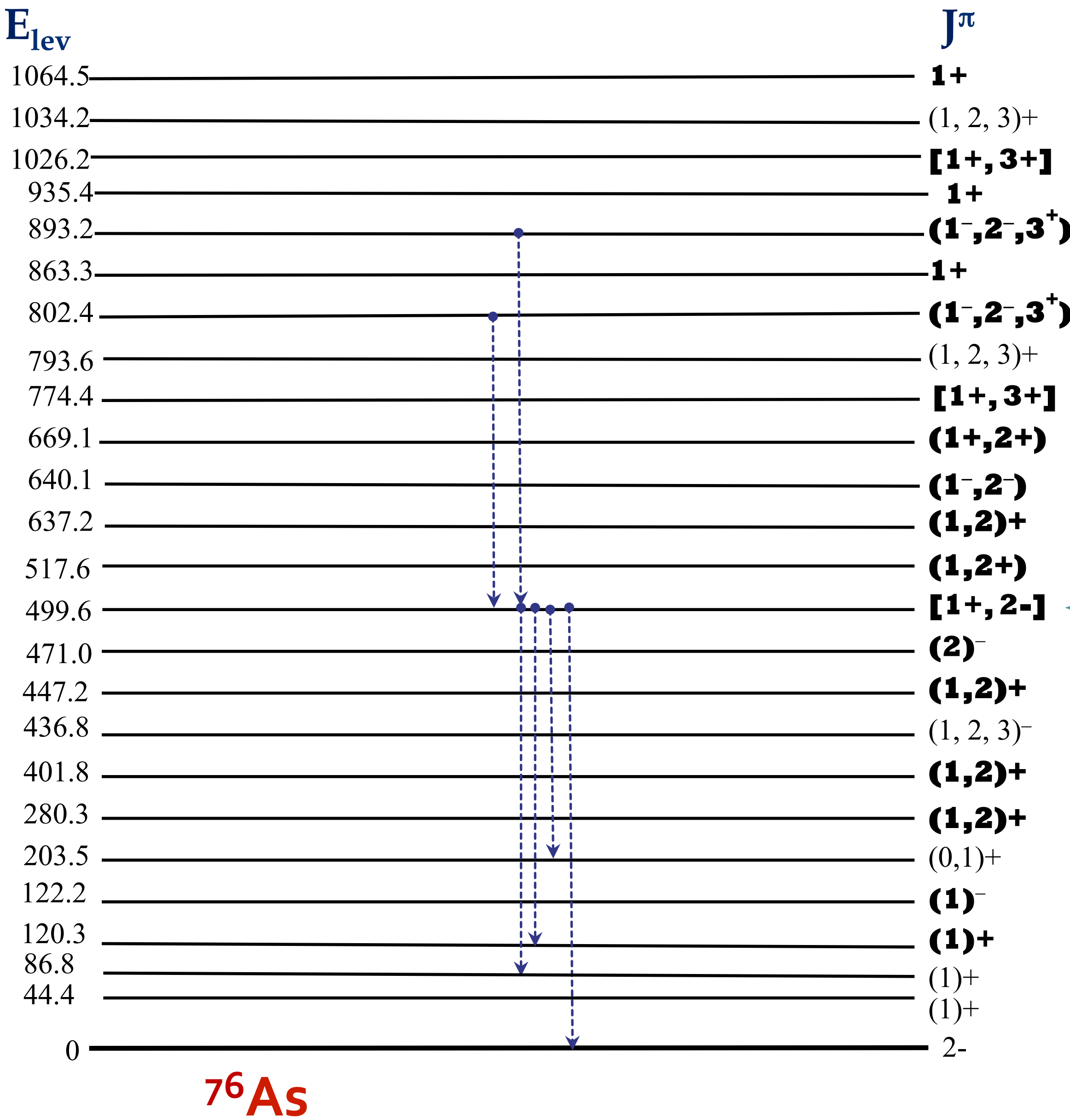

$$Y_j^{\mu} = \frac{\sum I_{i\downarrow}^{\gamma} - \sum I_i^{\gamma\downarrow}}{\varepsilon \sum_n I(K_n)}$$

$$P_j^{\mu}[\%] = \frac{\lambda_{part}}{\lambda_{cap}} \cdot 100\% = \frac{Y_j^{\mu}\lambda_{tot}}{\lambda_{cap}} \cdot 100\%$$

Partial μ-capture probabilities to ^{76}As

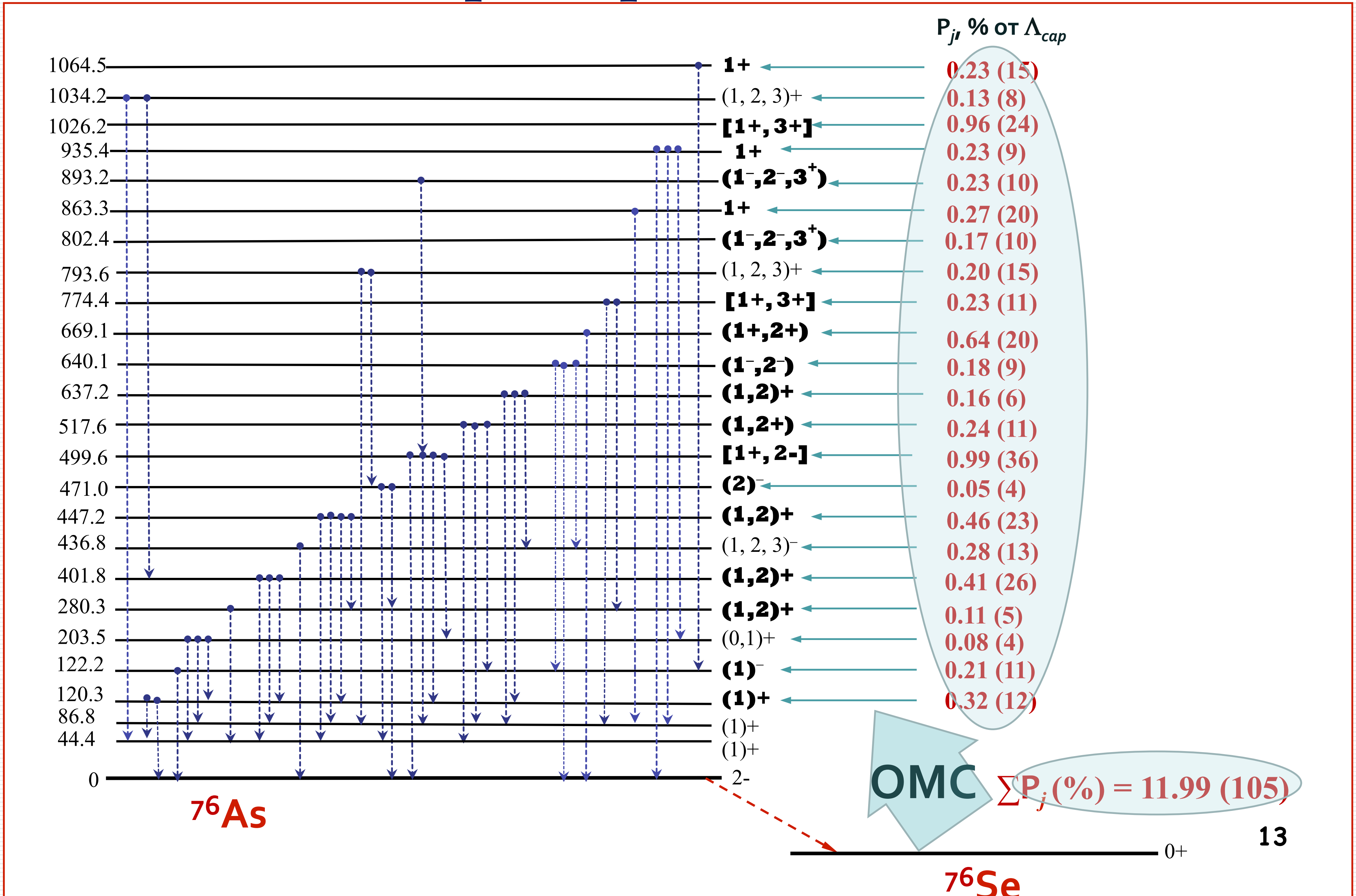

Partial μ-capture probabilities to ^{76}As

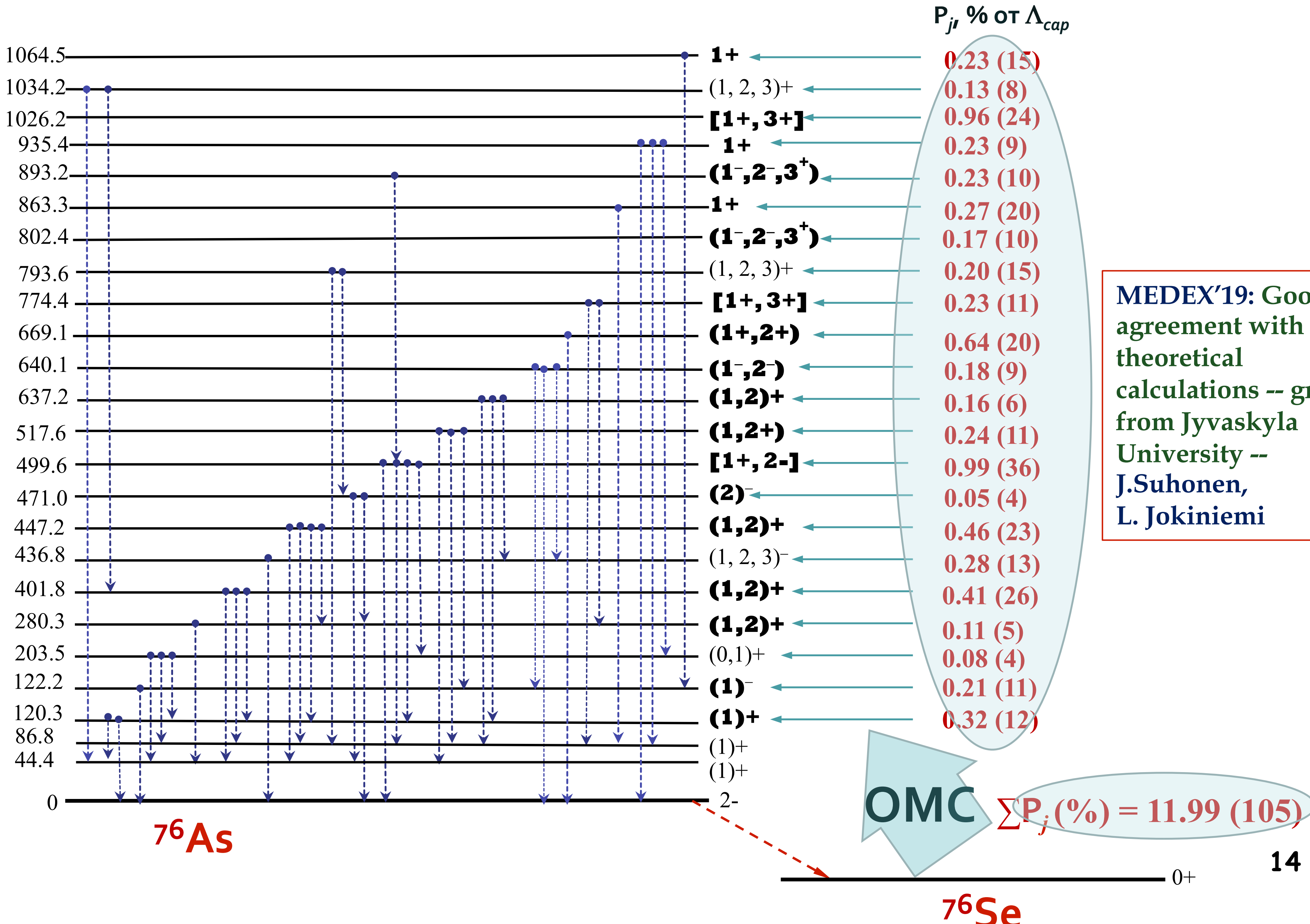

MEDEX'19: Good agreement with theoretical calculations -- group from Jyvaskyla University -- J.Suhonen, L. Jokiniemi

Results measured with U-spectra in ^{76}Se

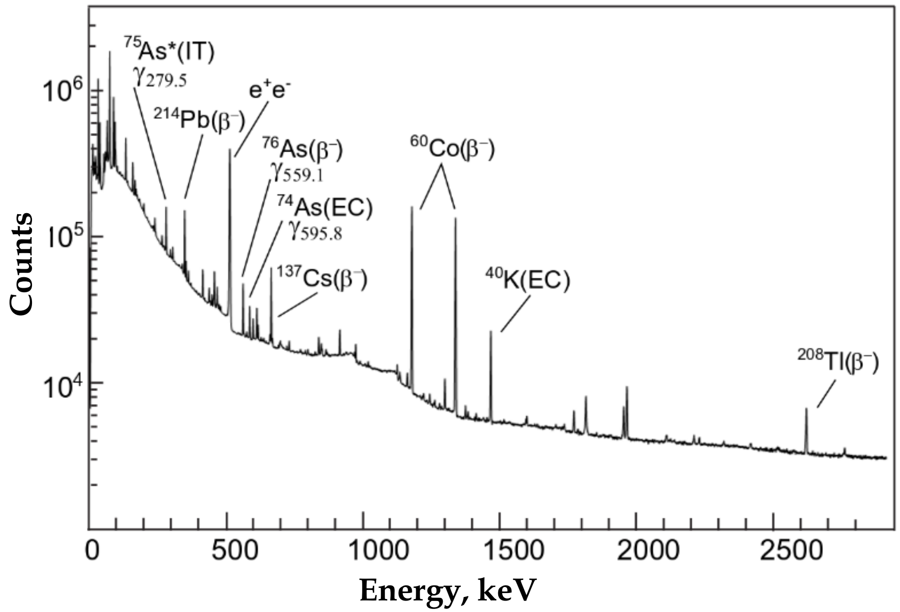

Isotope	Type of decay	$T_{1/2}$	Λ_{cap} (xn yp) [10^6 c^{-1}]	P_{cap} [%]
^{76}As	β^-	26.3 h	1.45(11)	13.65(255)
^{75m}As	IT	17.6 μs	1.80(31)	6.5(11)
^{75}As	stable		Not measured	
^{74}As	β^-, EC	17.8 d	1.1(2)	17.5(32)
^{73}As	EC	80.3 d	Not measured	
^{72}As	β^+	26 h	0.15(3)	2.4(5)
^{71}As	β^+	65.3 h	0.061(18)	0.96(28)
^{75m}Ge	IT	48 s	0.047(13)	0.75(21)
^{75}Ge	β^-	82.8 min	0.054(2)	0.86(3)
^{71m}Ge	IT	20 μs	0.020(3)	0.32(5)
^{74}Ga	β^-	8.1 min	0.026(6)	0.40(9)
^{72}Ga	β^-	14.1 h	0.026(7)	0.40(11)
				$\sum$=43.7(43)

Background radiation (**Uncorrelated** spectra) –

- calibration of the det-s,
- identification,
- yields of short-lived RI during exposure

Results measured with U-spectra in ^{76}Se

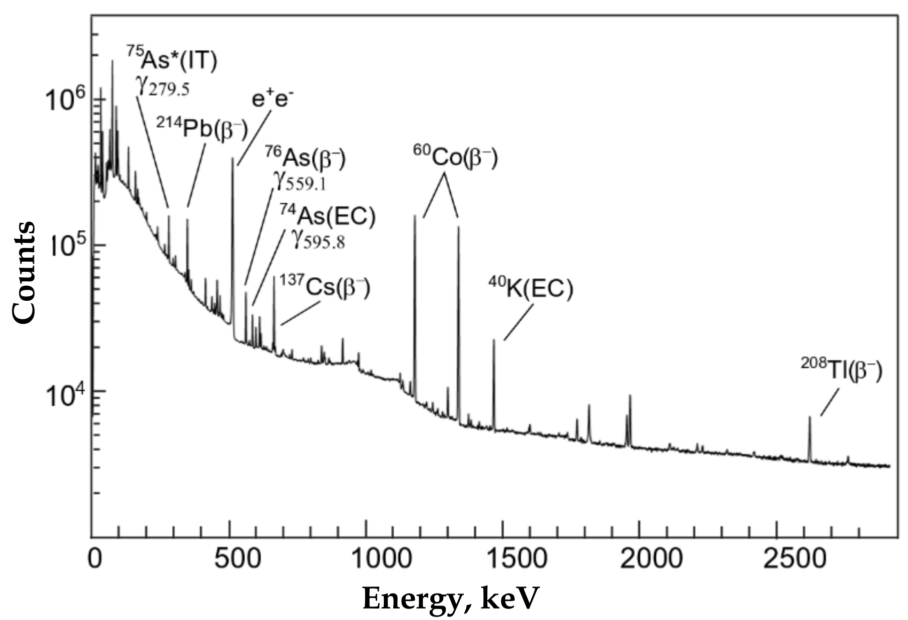

Isotope	Type of decay	$T_{1/2}$	Λ_{cap} (xn yp) [10^6 c^{-1}]	P_{cap} [%]
^{76}As	β^-	26.3 h	1.45(11)	13.65(255)
^{75m}As	IT	17.6 μs	1.80(31)	6.5(11)
^{75}As	stable		Not measured	
^{74}As	β^-, EC	17.8 d	1.1(2)	17.5(32)
^{73}As	EC	80.3 d	Not measured	
^{72}As	β^+	26 h	0.15(3)	2.4(5)
^{71}As	β^+	65.3 h	0.061(18)	0.96(28)
^{75m}Ge	IT	48 s	0.047(13)	0.75(21)
^{75}Ge	β^-	82.8 min	0.054(2)	0.86(3)
^{71m}Ge	IT	20 μs	0.020(3)	0.32(5)
^{74}Ga	β^-	8.1 min	0.026(6)	0.40(9)
^{72}Ga	β^-	14.1 h	0.026(7)	0.40(11)
				$\sum$=43.7(43)

Background radiation (**Uncorrelated** spectra) –

- calibration of the det-s,
- identification,
- yields of short-lived RI during exposure

$0\nu2\beta$ -decay	$0\nu2\beta$ -experiments	OMC targets	Status
^{76}Ge	GerdaI/II, Majorana Demonstrator	^{76}Se	Total and partial capture rates, RI yields
^{48}Ca	TGV, NEMO3, Candles III	^{48}Ti	Total and partial capture rates
^{106}Cd	TGV	^{106}Cd	Total and partial capture rates
^{82}Se	NEMO3, SuperNEMO, Lucifer(R&D)	^{82}Kr	Total capture rates (PSI, 2019)
^{100}Mo	NEMO3, AMoRE(R&D), LUMINEU(R&D)	^{100}Ru	-
^{116}Cd	NEMO3, Cobra	^{116}Sn	-
^{150}Nd	SuperNEMO, DCBA(R&D)	^{150}Sm	Total capture rates, RI yields
^{136}Xe	EXO200, Kamland-Zen, NEXT	^{136}Ba	2020 (RCNP)
^{130}Te	Cuore 0/Cuore, SNO+	^{130}Xe	2019 (PSI)

Link: muxrays.jinr.ru

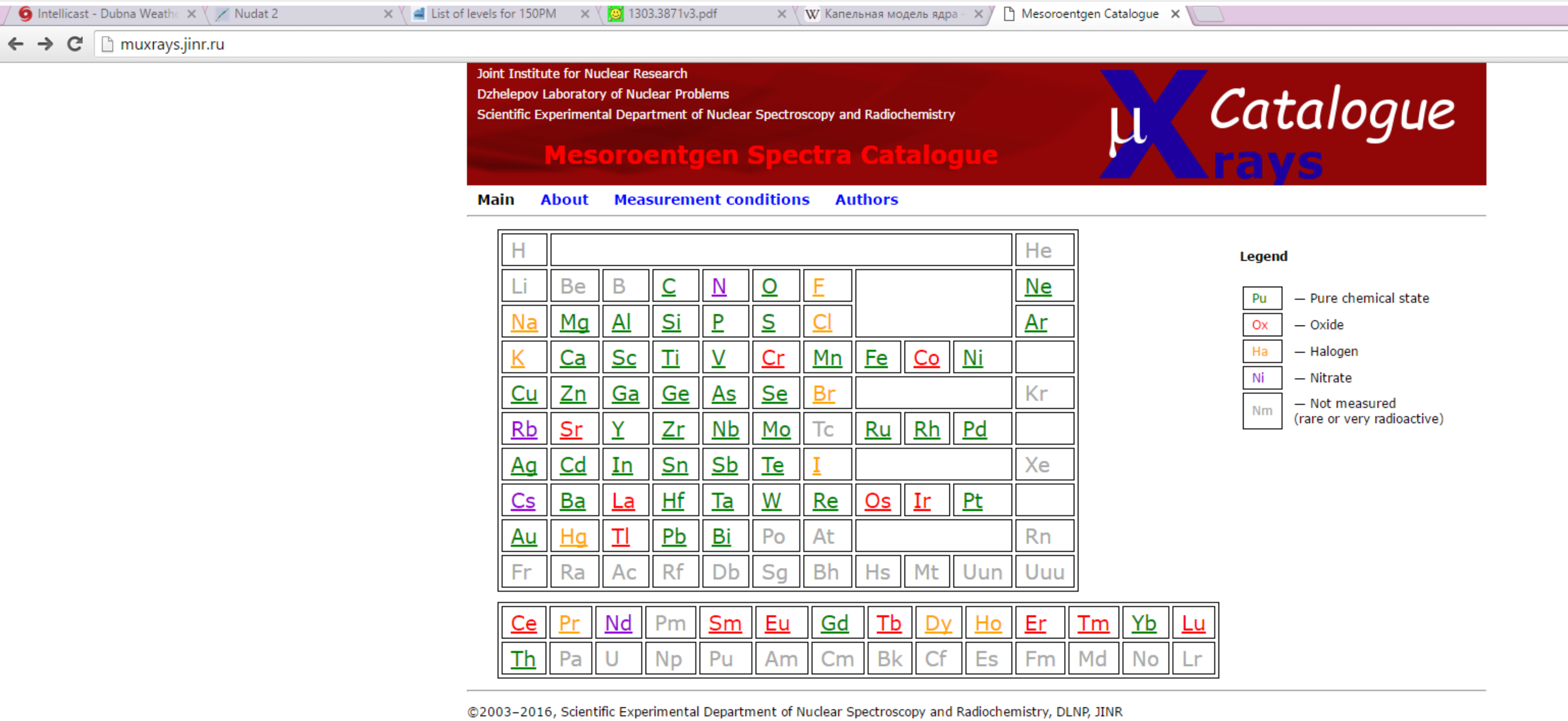

The information from the μX-ray spectra catalogue is important! (It helps us to identify γ-lines, background, and gives correct selection of the targets and construction materials for different experiments with muons)

Angular correlations with ν in OMC
(Doppler shape of γ-lines)

^{20}Ne, ^{12}C and ^{16}O were investigated for that purpose

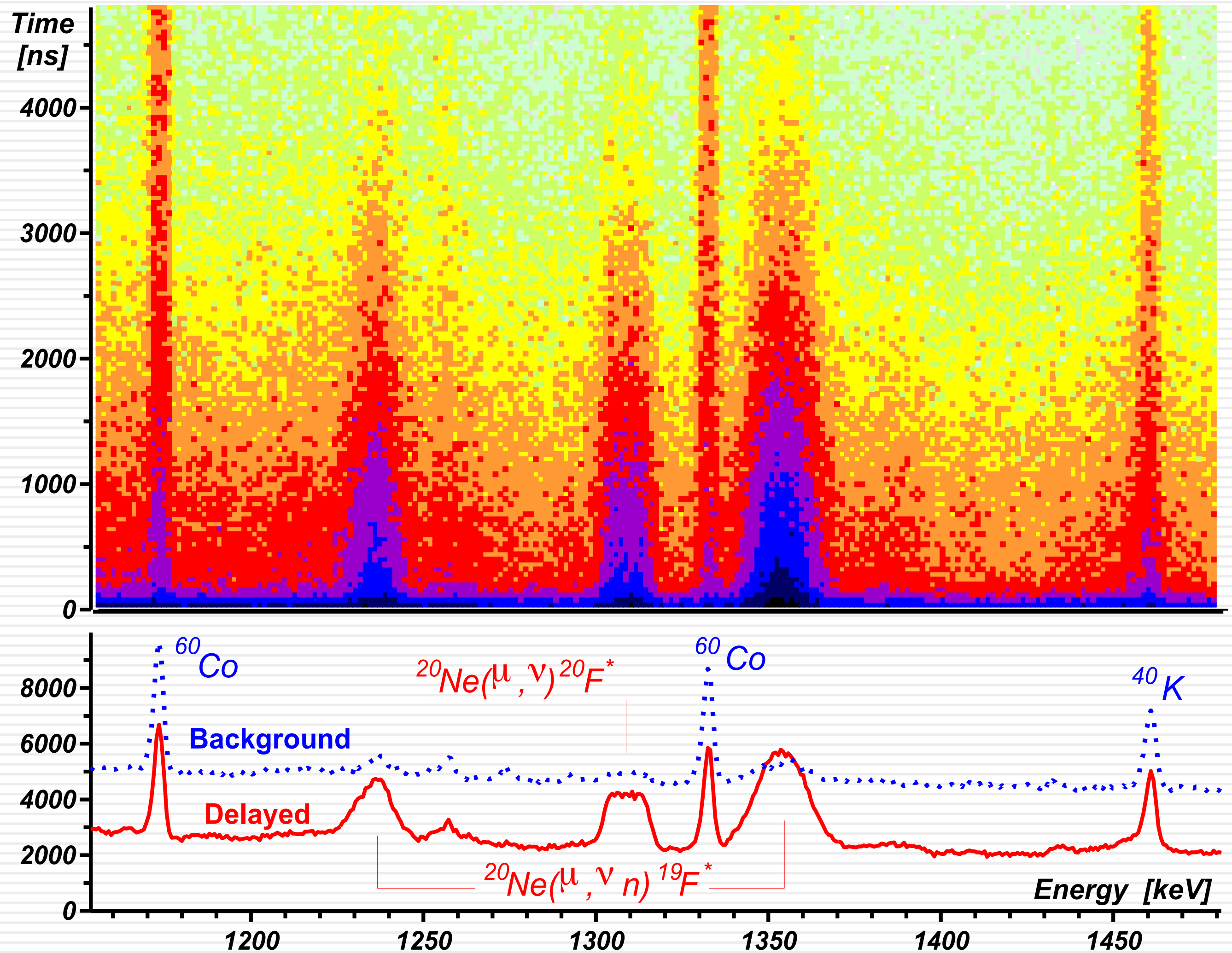

Conclusions:

- **OMC presently seems to be a bit off the main stream of physics**

But: it can provide important information about the high-q component of the weak nuclear response, i.e. it is relevant for the neutrinoless double beta decay (and astrophysics)

- **Several targets (^{48}Ti, ^{76}Se, ^{82}Kr, ^{106}Cd, ^{150}Sm) have been studied by our group for the double beta decay (^{48}Ca, ^{76}Ge, ^{82}Se ^{106}Cd, ^{150}Nd).** Total and Partial capture rates were extracted and a substantial strength of the μ -capture was found to reside in the low-energy region -- especially in the case of heavy systems.
  D. Zinatulina et al. **Phys. Rev. C 99 (2019) 024327**
  PhD thesis of D.Zinatulina
- By-product: Electronic catalogue of muonic X-rays have been made (muxrays.jinr.ru)
- **Angular correlations for ^{20}Ne, ^{16}O and ^{12}C have been investigated (g_p/g_A, PCAC)**
- Further theoretical efforts is be needed
- **New initiatives are very welcome to advance**

UTM
UNIVERSITI TEKNOLOGI MALAYSIA

RCNP

JOINT INSTITUTE
FOR NUCLEAR RESEARCH

Thank you for your attention!

PAUL SCHERRER INSTITUT
PSI

JYVÄSKYLÄN YLIOPISTO
UNIVERSITY OF JYVÄSKYLÄ

Back Slides

Total μX-ray spectrum of Cd

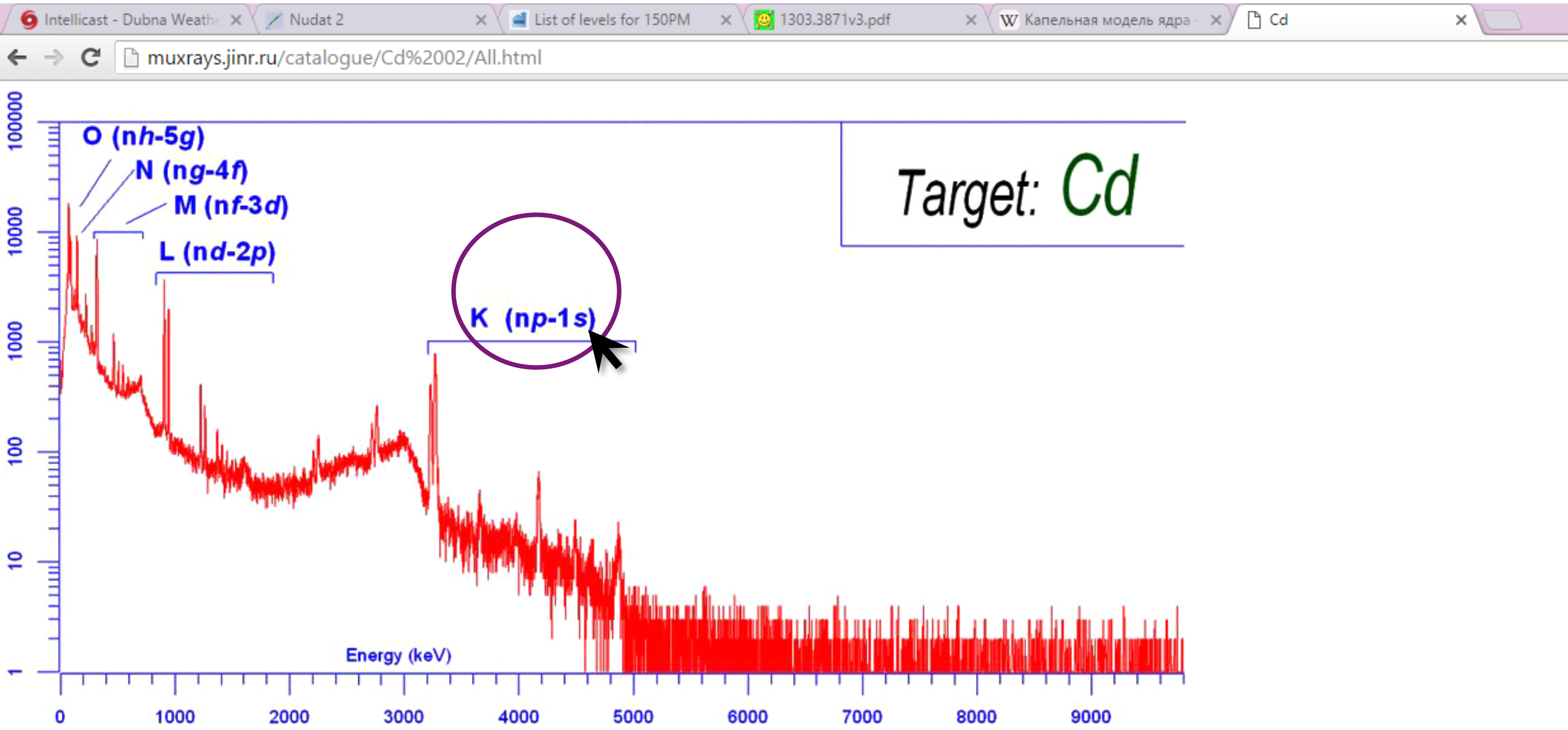

Ordinary Muon Capture (OMC)

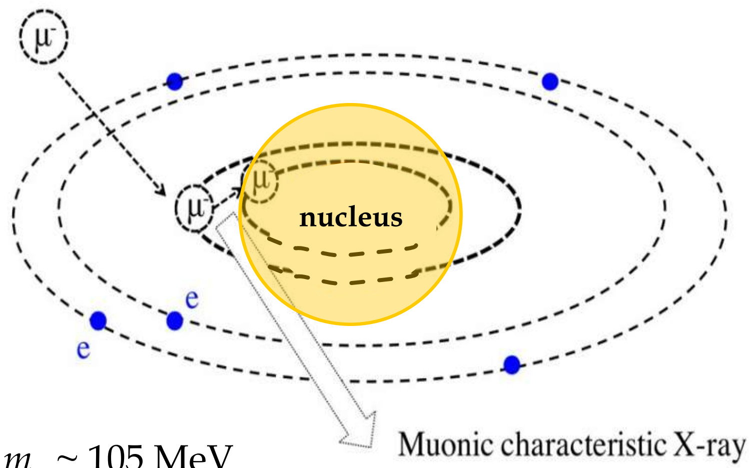

$m_\mu \sim 105$ MeV

$\mu^- \rightarrow e^- + \nu_e + \nu_\mu \qquad \tau_{dec} = 2.2\mu s$

$(A, Z) + \mu^- \rightarrow (A, Z\text{-}1)^* + \nu_\mu$

$\rightarrow (A, Z\text{-}1) + \gamma$

$\rightarrow (A\text{-}1, Z\text{-}1) + \gamma + n$

$\rightarrow (A\text{-}2, Z\text{-}1) + \gamma + 2n$

$\rightarrow (A\text{-}1, Z\text{-}2) + \gamma + n + p$

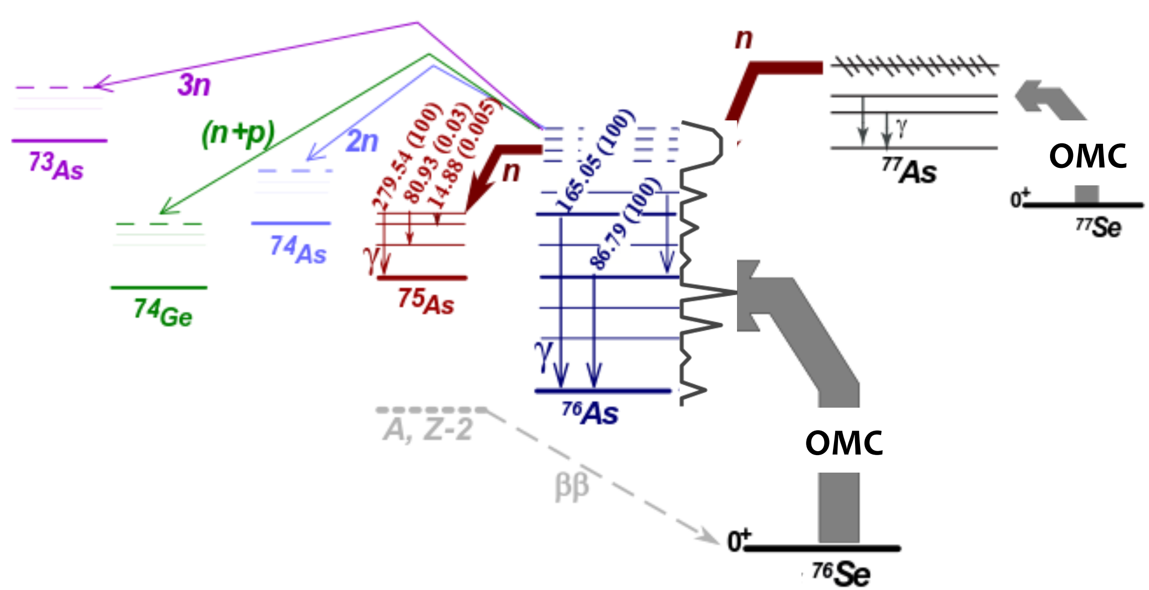

- Muonic characteristic X-rays (normalization, identification)
- γ-radiation following OMC in targets (total and partial capture rates)
- Yields of short-lived RI during exposure

- PhD thesis of D.Zinatulina
- [1] D. Zinatulina et al. **Phys. Rev. C 99 (2019) 024327**

Ordinary muon capture studies for the matrix elements in $\beta\beta$ decay

D. Zinatulina,[1] V. Brudanin,[1] V. Egorov,[1] C. Petitjean,[2] M. Shirchenko,[1] J. Suhonen,[3] and I. Yutlandov[1]

[1] *Joint Institute for Nuclear Research, 141980 Dubna, Russia*
[2] *Paul Scherrer Institute, 5232 Villigen, Switzerland*
[3] *Department of Physics, University of Jyväskylä, PO Box 35, FIN-40351 Jyväskylä, Finland*

(Dated: October 16, 2018)

Precise measurement of γ-rays following ordinary (non-radiative) capture of negative muons by natural Se, Kr, Cd and Sm, as well as isotopically enriched ^{48}Ti, ^{76}Se, ^{82}Kr, ^{106}Cd and ^{150}Sm targets was performed by means of HPGe detectors. Energy and time distributions were investigated and total life time of negative muon in different isotopes was deduced. Detailed analysis of γ-lines intensity allows to extract relative yield of several daughter nuclei and partial rates of (μ,ν) capture to numerous excited levels of the ^{48}Sc, ^{76}As, ^{82}Br, ^{106}Ag and ^{150}Tc isotopes which are considered to be virtual states of an intermediate odd-odd nucleus in 2β-decay of ^{48}Ca, ^{76}Ge, ^{82}Se, ^{106}Cd and ^{150}Nd, respectively. These rates are important as an experimental input for the theoretical calculation of the nuclear matrix elements of 2β-decay.

PACS numbers: 23.40.-s, 23.40.Hc, 27.40.+z, 27.50.+e, 27.60.+j, 27.70.+q

I. INTRODUCTION

At the moment the neutrinoless $\beta\beta$ ($0\nu\beta\beta$) decay of atomic nuclei is the only practical means of accessing the Majorana nature of the neutrino. In order to occur the decay requires the violation of lepton-number conservation and non-zero neutrino mass. Due to the importance of the related beyond-the-standard-model physics it is of interest to study the nuclei involved by both experimental and theoretical means. Large experimental collaborations have been established in order to measure the $0\nu\beta\beta$ half-lives in the presently running and future underground experiments. The connection between the (possibly) measured half-lives and the fundamental observables, like the electron neutrino mass, is provided by the nuclear matrix elements (NMEs) [1].

Nuclear models aimed at the description of the NMEs of $0\nu\beta\beta$ decays have traditionally been tested in connection with the two-neutrino $\beta\beta$ ($2\nu\beta\beta$) decays [1, 2] and β decays [3]. In [4] it was proposed that the ordinary muon capture (OMC) could be used for this purpose, as well. The $2\nu\beta\beta$ and β decays are low-momentum exchange processes ($q \sim$ few MeV), whereas both $0\nu\beta\beta$ and OMC are high-momentum exchange processes ($q \sim 100$ MeV). In this way the $0\nu\beta\beta$ and OMC are similar processes and possess similar features: they are able to excite high-lying nuclear states with multipolarities J^π higher than $J^\pi = 1^+$. The $0\nu\beta\beta$ decay proceeds between the 0^+ ground states of parent and daughter even-even nuclei through virtual states of the intermediate odd-odd nucleus. These same virtual states can be accessed by the OMC from either the daughter nucleus (electron emitting

the processes stemming, e.g., from the neutrino potential generated by the propagator of the virtual Majorana neutrino in the $0\nu\beta\beta$ decay [5]. Despite this difference the OMC can effectively probe the nuclear wave functions relevant for the $0\nu\beta\beta$ decay, as shown for the light nuclei in the shell-model framework in [6].

For the medium-heavy and heavy open-shell nuclei the shell-model framework is unfeasible due to computational limitations. For these nuclei the model framework of the quasiparticle random-phase approximation (QRPA [7] is a good choice. In particular, the proton-neutron version of the QRPA (pnQRPA) can access the virtual intermediate states of the $0\nu\beta\beta$ decays [1]. A particular problem pestering the pnQRPA approach is the uncertainty associated with one of its key parameters, the particle-particle interaction strength $g_{\rm pp}$. This parameter is used to introduce a phenomenological overall scaling of the particle-particle part of proton-neutron interaction [8]. It is not clear how this scaling should be done for the $0\nu\beta\beta$ decays since there is no experimental data for transitions from either the $0\nu\beta\beta$ mother or daughter nuclei to the multipole $J^\pi \neq 1^+, 2^-$ intermediate states (the 1^+ and partly 2^- states can be probed by the (p,n) and (n,p) charge-exchange reactions [9]). In this case the only viable method to access this "$g_{\rm pp}$ problem" is the OMC [10]. By using experimental data on OMC to individual intermediate J^π states one can access the value of $g_{\rm pp}$ for each multipole separately and at the same time study the consistency of these values by comparison with the measured OMC rates for a wider palette of nuclear states.

In order to give an experimental input to 2β NME cal-

arXiv: 1803.10960v2

URL: http://muxrays.jinr.ru/

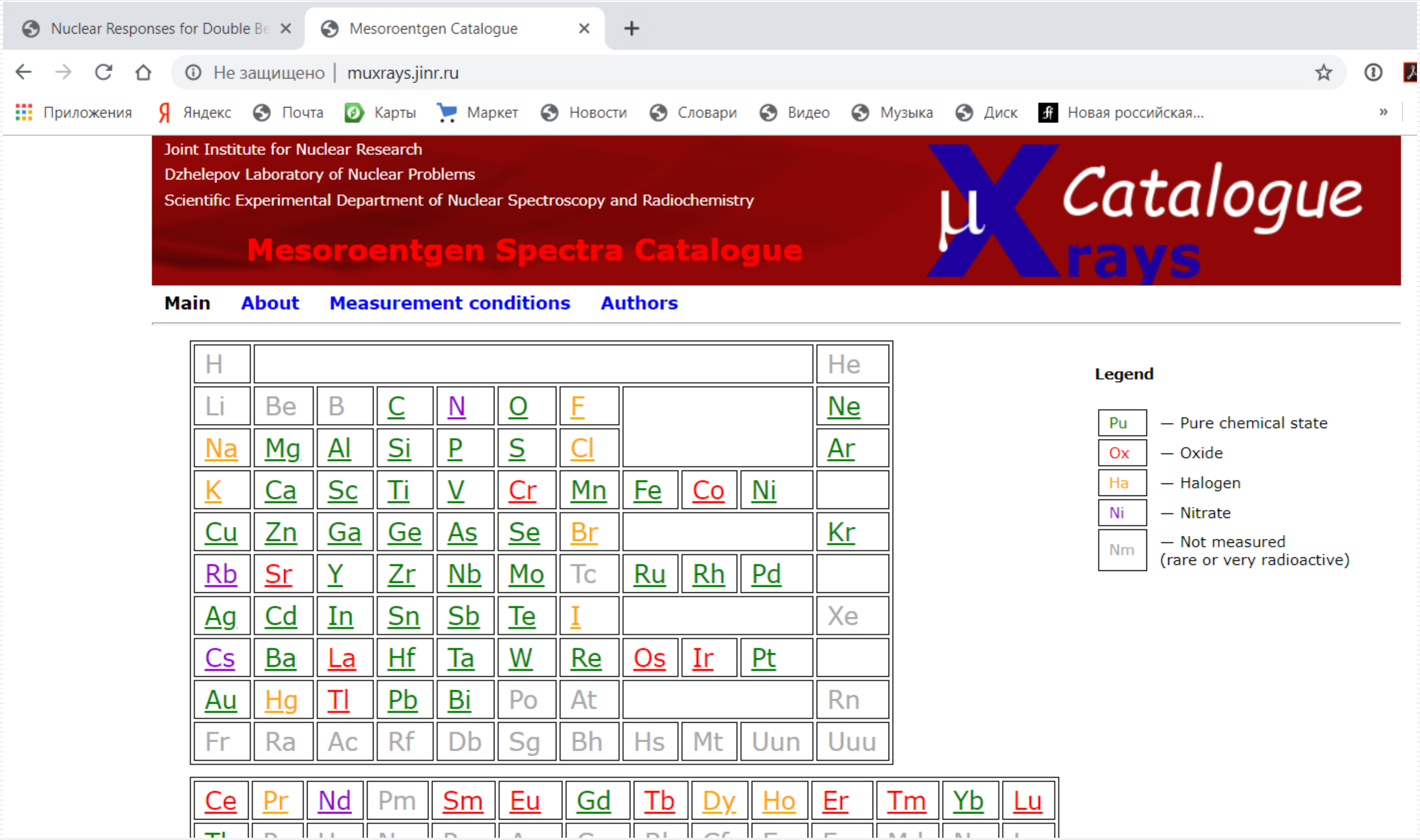

Измерено более 75 химических элемент

Total μX-ray spectrum of Cd

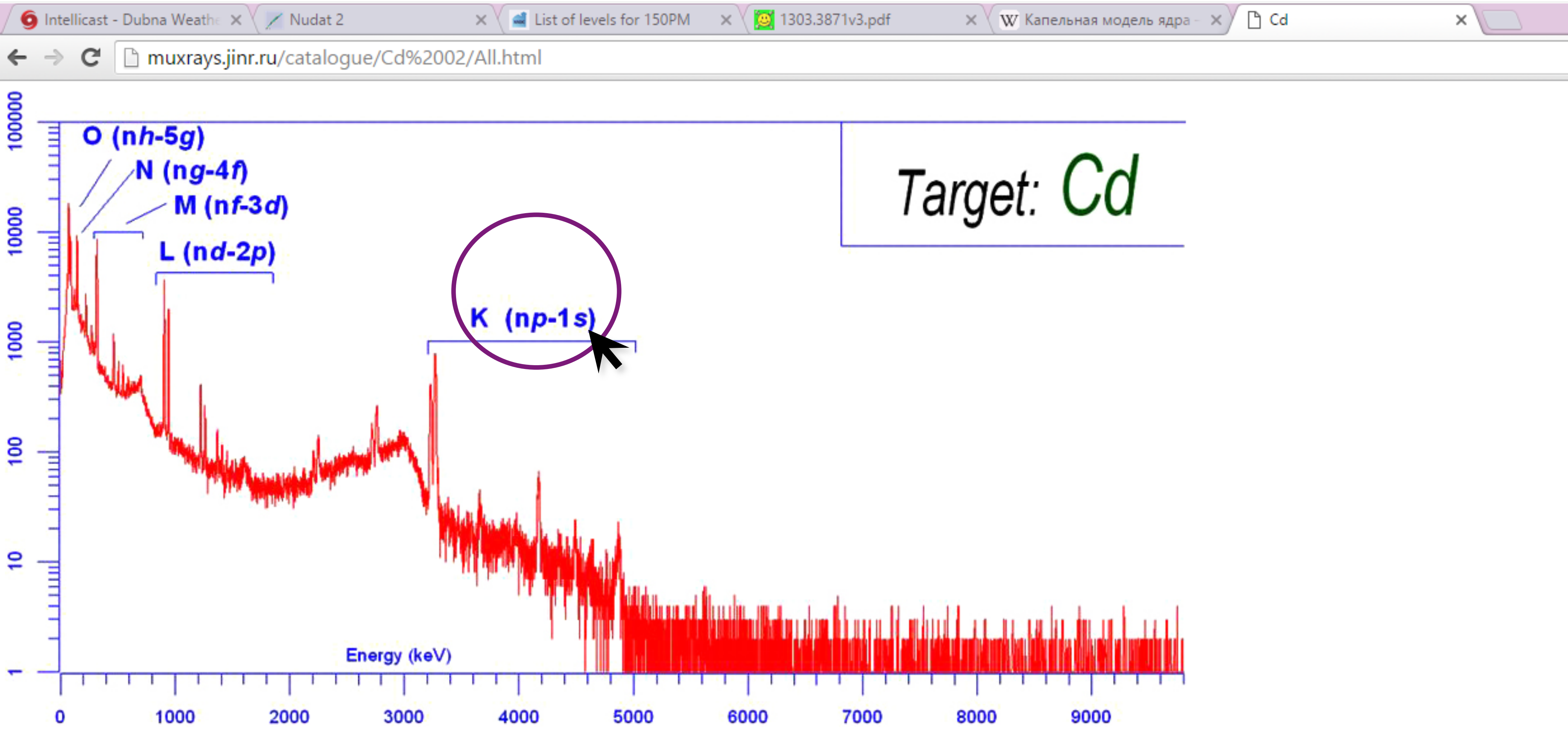

Статус по ЯМЭ. Подавление g_A параметра (Й. Сухонен и др.,Ювяскюля)

$$(T^{0\nu}_{1/2})^{-1} = \left(\frac{\langle m_\nu \rangle}{m_e}\right)^2 \times F_{0\nu} \times |\mathrm{NME}_{0\nu}|^2$$

$$|\mathrm{NME}_{0\nu}|^2 \cong \left|M^{0\nu}_{GTGT}\right|^2 = (g_{a,0\nu})^4 \left|\Sigma_{J^\pi}(\langle 0_f^+ | O^{0\nu}_{GTGT} | 0_i^+ \rangle)\right|^2$$

^{76}Ge

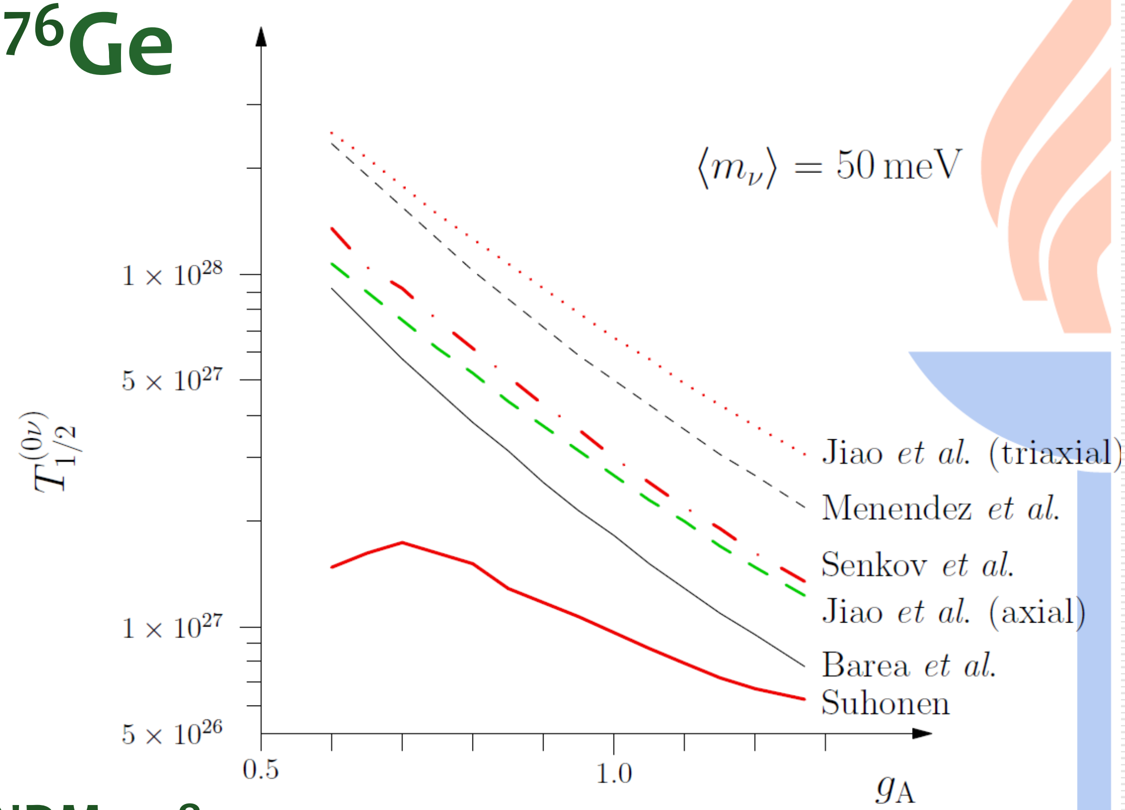

Jiao et al.: Phys.Rev. C 96 (2017) 054310 (GCM+ISM)

Menendez et al.:Nucl. Phys. A 818 (2009) 139 (ISM)

Senkov et al.:Phys. Rev. C 93 (2016) 044334 (ISM)

Barea et al.: Phys.Rev. C 91 (2015) 034304 (IBM-2)

Suhonen: Phys.Rev. C 96 (2017) 055501 (pnQRPA+ isospin restoration + data on 2νββ)

Расчеты с использованием оболочечной модели (^{56}Fe, ^{24}Mn, ^{32}S)

- Кандидаты DBD
- Проверка подавления g_A
- Вклад V,A,P в парциальные скорости захвата

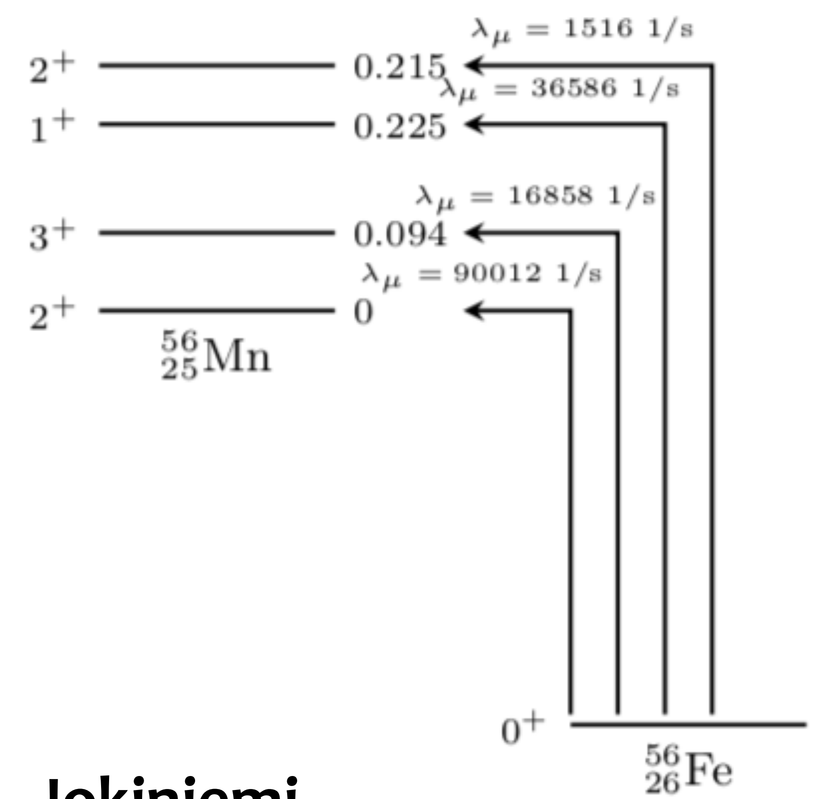

L. Jokiniemi

$$\lambda_\mu \approx C(q_i) \sum_{\kappa u} |g_V M_V(\kappa,u) + g_A M_A(\kappa,u) + g_P M_P(\kappa,u)|^2$$

Ускоритель RCNP и E489 эксперимент

RCNP

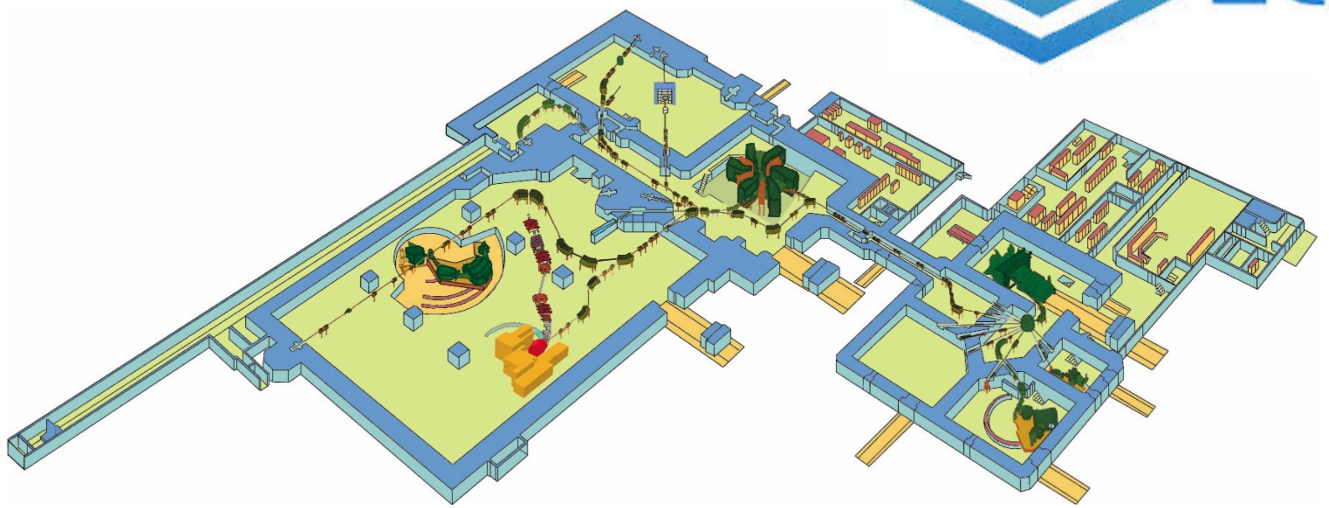

BEAM LINE: MuSIC

BEAM REQUIREMENTS:

Type of particle	proton
Beam energy	400 MeV
Beam intensity	1 μA
Type of particle	muon
Muon momentum	50 MeV/c
Beam intensity	1 μA

PRC 97(2018) 014617 (J-PARC 2014)

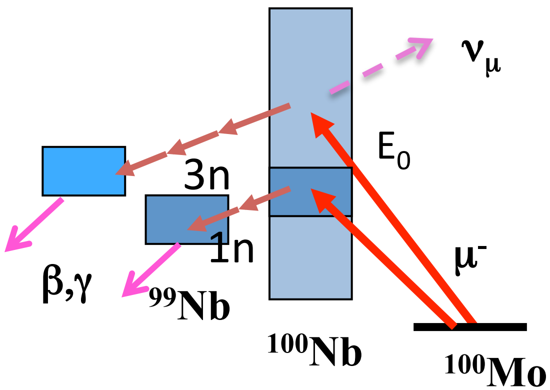

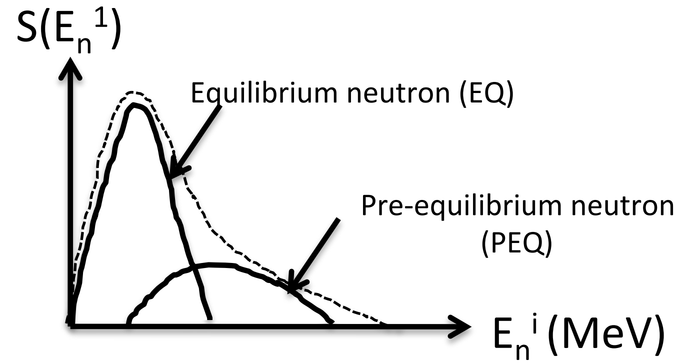

$$S(E_n^1) = k\left[E_n^1 exp\left(-\frac{E_n^1}{T_{\mathrm{EQ}}(E)}\right) + pE_n^1 exp\left(-\frac{E_n^1}{T_{\mathrm{PEQ}}(E)}\right)\right]$$

{EQ} {PEQ}

μ response(strength) distribution

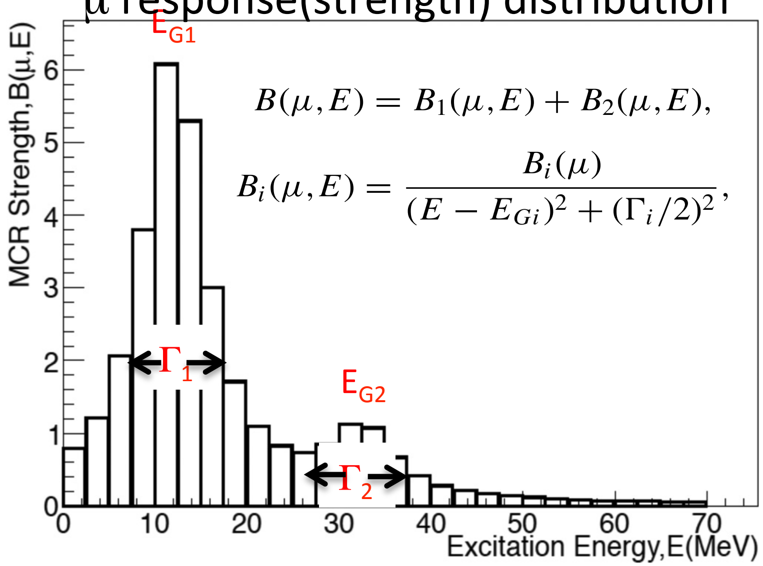

FIG. 6. The OMC strength distribution suggested from the experimental RI distribution. E_{G1} and E_{G2} are the OMC GRs at around 12 MeV and 30 MeV.

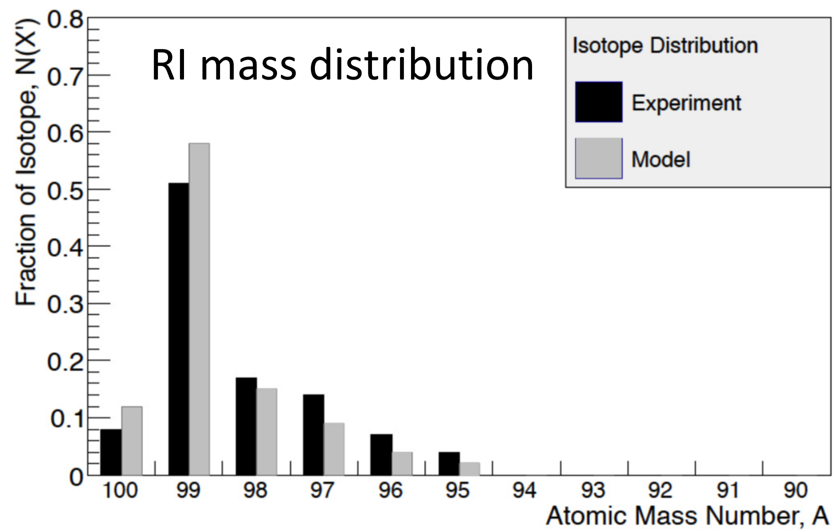

Overview of the method

Irradiation of target

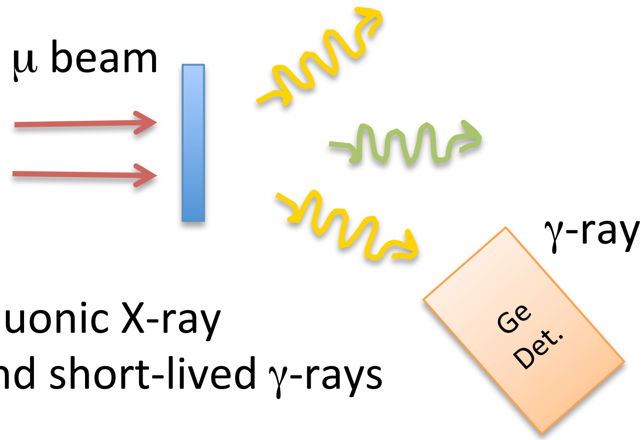

muonic X-ray and short-lived γ-rays

Measurement of delayed γ-rays

$^{100}Mo + \mu^- \rightarrow Nb^* + \nu_\mu + xn$

$\rightarrow Nb^* + \beta^- + \overline{\nu}_e + \gamma$

Exp. data give the dist. of isotope mass population of the final nuclei after neutron emission.

Muon capture reaction

Weak/ neutrino nuclear response

compare

Calculation by proton and neutron emission model

Provides initial capture strength ^{100}Nb after muon capture

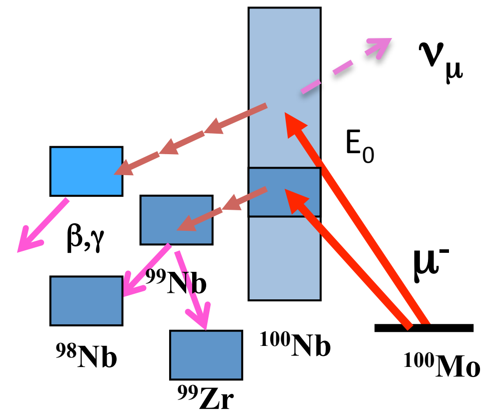

Distribution of initial strength can provide the final nuclei isotope population

Relative capture strength

- Provide μ capture rate
- If pnQRPA with g_A can reproduce the μ capture rate or they need to adjust g_A.

Absolute capture strength

Nuclear matrix element, NME for DBD

- Used adjusted g_A to calculate DBD NME

E489 эксперимент (февраль 2018г.)

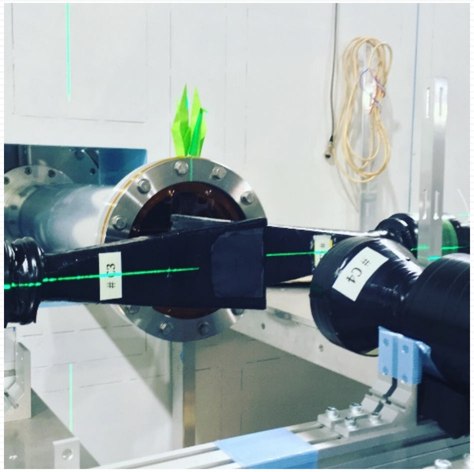

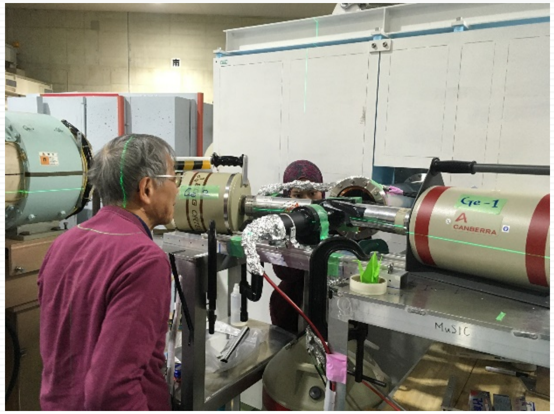

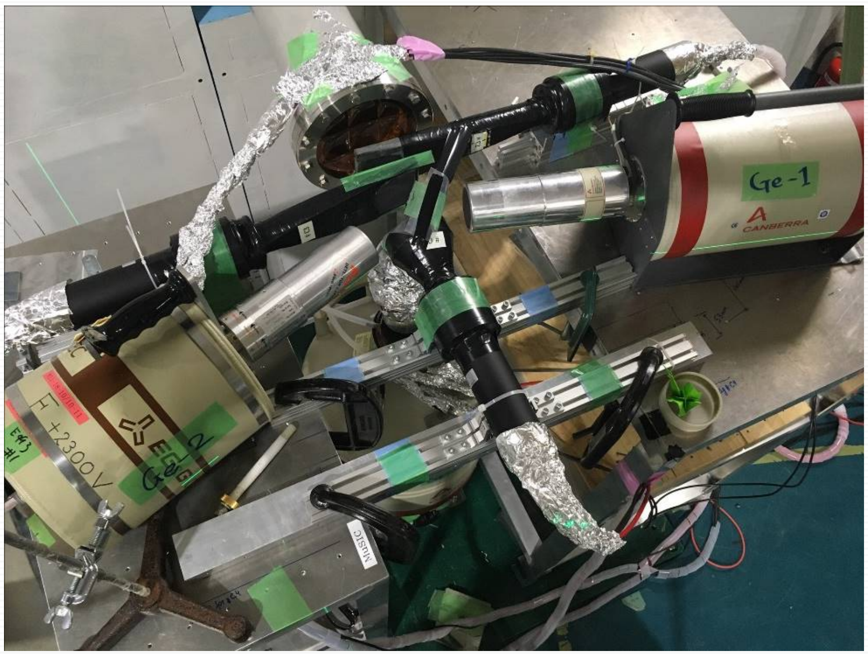

E489 коллаборация:

I.H. Hashim [1], D .Zinatulina[3],
H. Ejiri[2], A.Sato[2], M. Shirchenko[3], S.A.Hamzah[1],
F.Othman[2], K.Ninomiya[2], T.Shima[2], K. Takahisa[2],
D.Tomono[2], Y.Kawashima[2] and V. Egorov[3]

[1] Технический Университет Малайзии, Скудай, Малайзия
[2] Центр исследования ядерных проблем, Япония, Осака
[3] Объединенный Институт Ядерных Исследований, Россия, Дубна

Detector efficiencies and timing

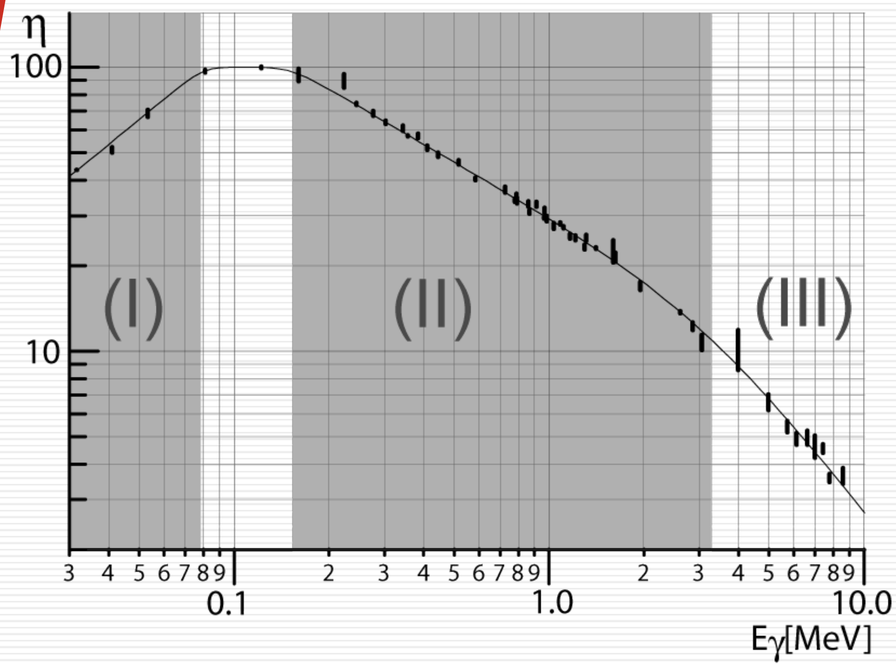

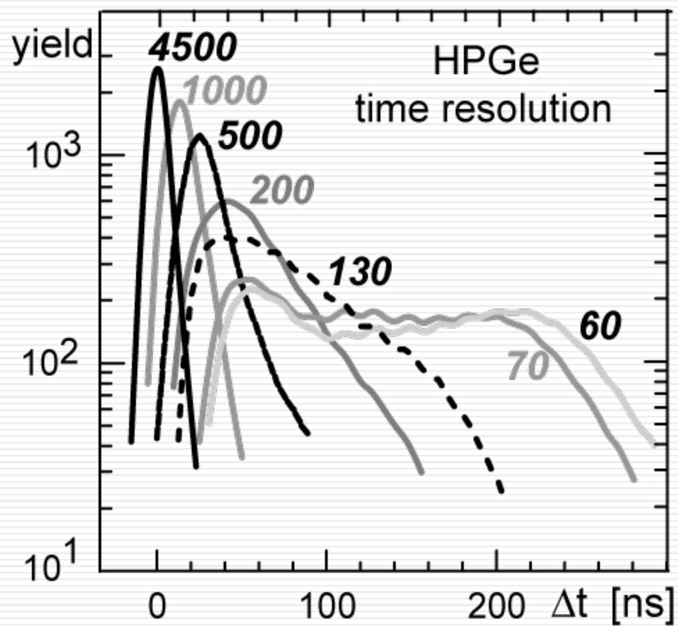

high γ's from
$^{35}Cl(n,\gamma)$, $^{56}Fe(n,\gamma)$, $^{28}Si(n,\gamma)$
and
μX-rays from Au, Cd, Sm

timing deterioration due co-axial geometry of HPGe
time lag due to incomplete charge collection

URL: http://muxrays.jinr.ru/

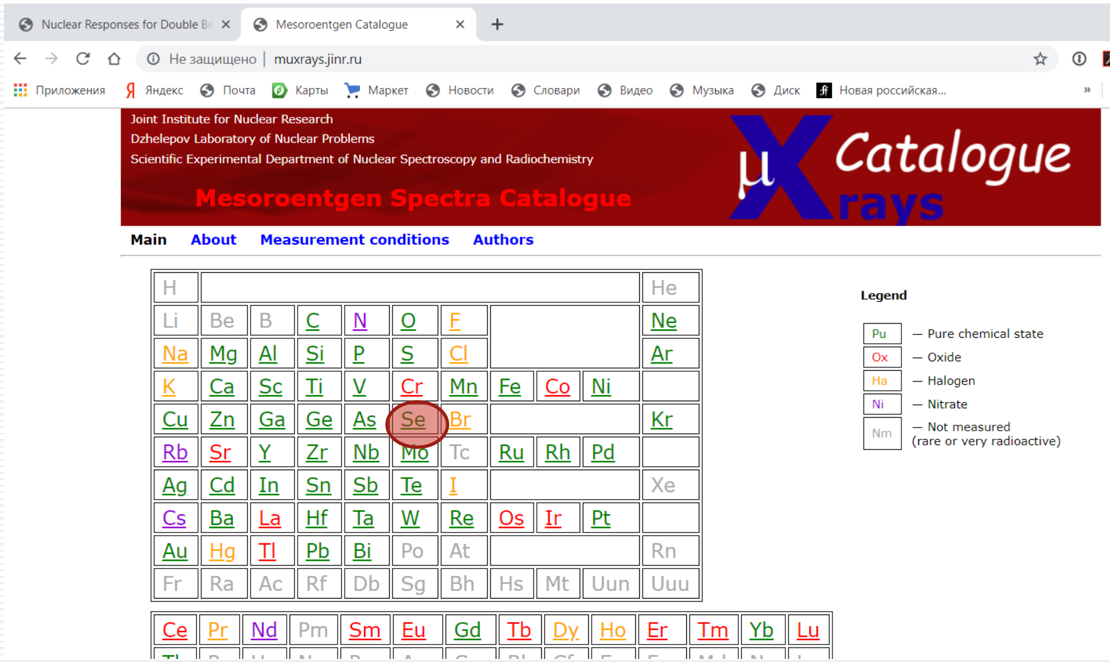

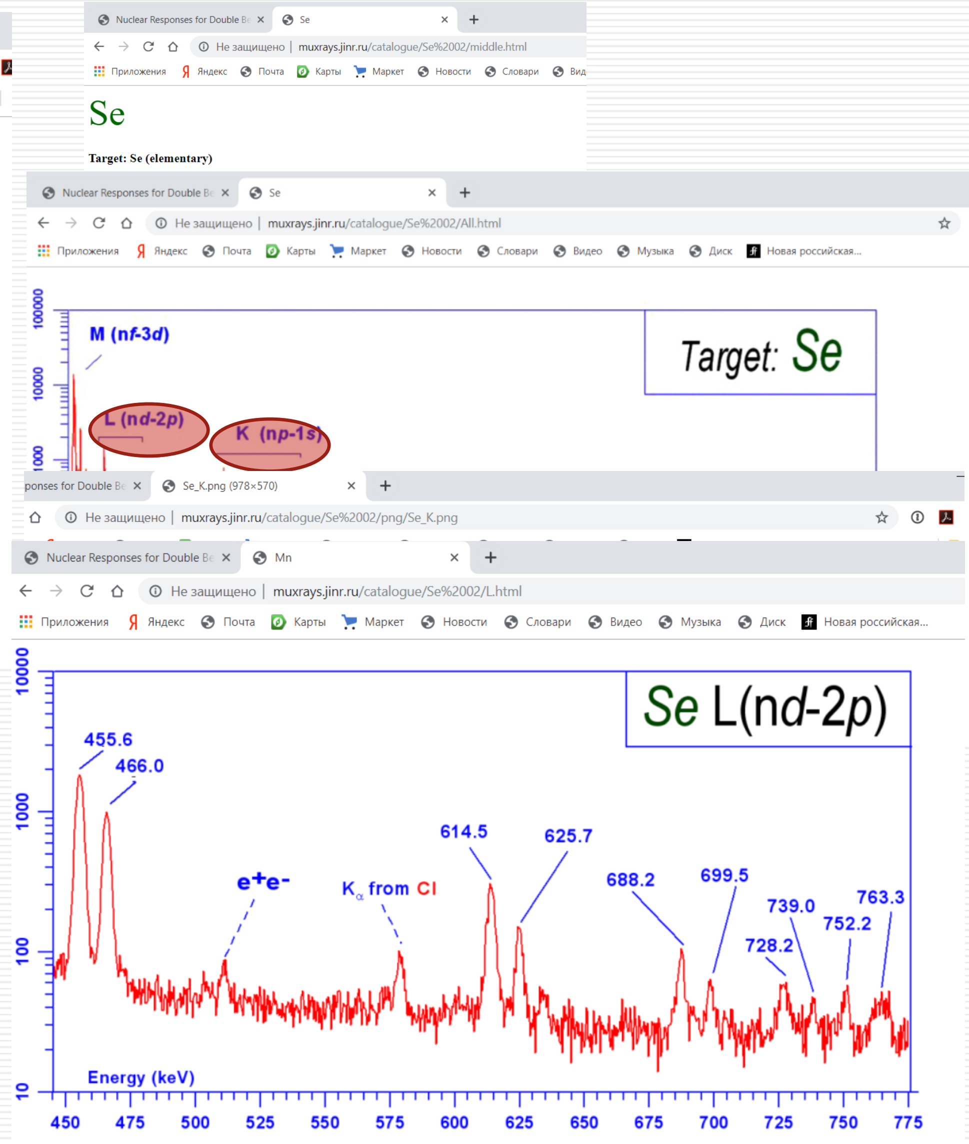

Измерено более 75 химических элемент

Метод временнóй эволюции γ-линии

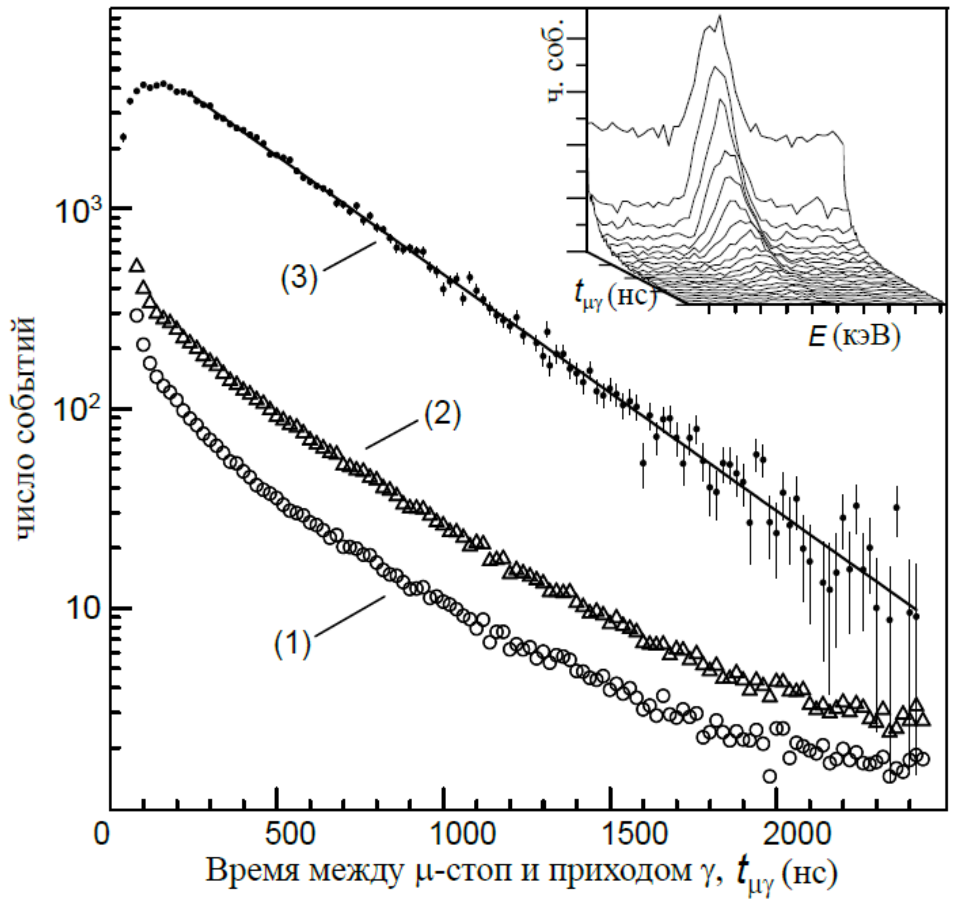

Временнáя эволюция фрагмента (врезка) γ-линии 227 кэВ, сопровождающей ОМЗ в ^{48}Ti.

Полная скорость исчезновения мюона:

$$\Lambda_{tot} = 1/\tau = \Lambda_{cap} + H \cdot \Lambda_{free} + \ldots,$$

Λ_{free} – распад свободного мюона, H – фактор Хаффа,

$$\Lambda_{cap} = \Lambda_{cap}(0n) + \Lambda_{cap}(1n) + \Lambda_{cap}(2n) + \Lambda_{cap}(1p) + ..$$

(1) – центральная часть фрагмен + фон под ней) – 1 ч;

(2) – фоновая часть вокруг энерг (1 ч);

(3) – область γ-линии (фитировани Гаусса с пятью параметрами и временного отрезка) – 73 ч.

$$f(t) = A_1 \cdot Exp(-t/\tau) + C^0$$

Различная форма γ-линий в Ne. Угловые корреляции.

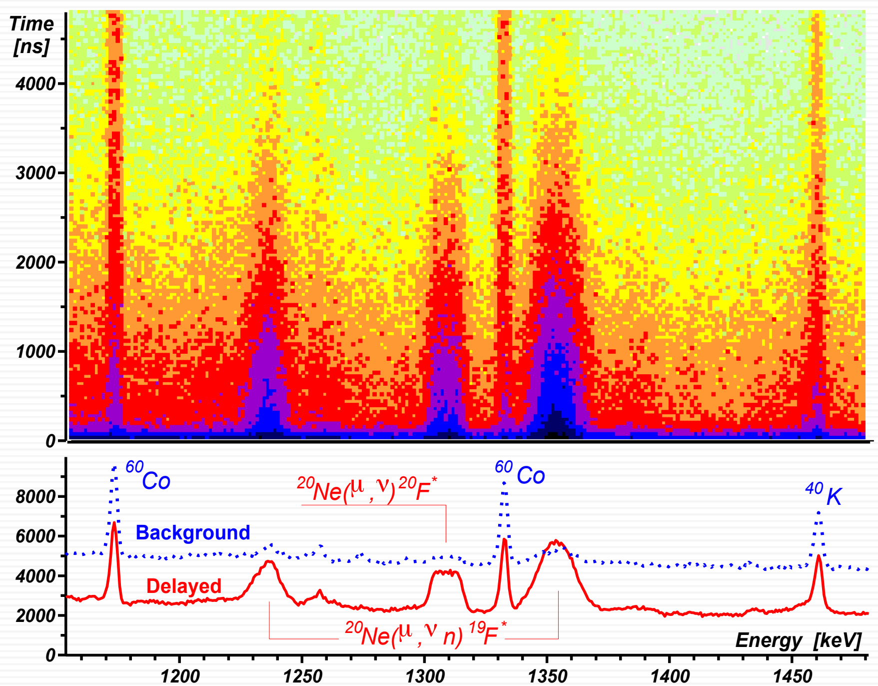

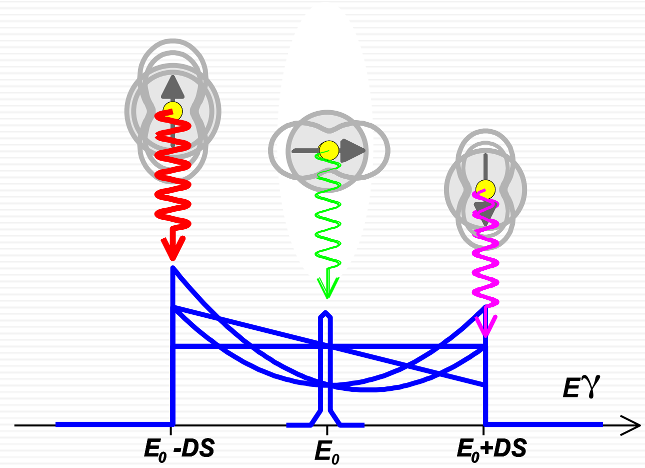

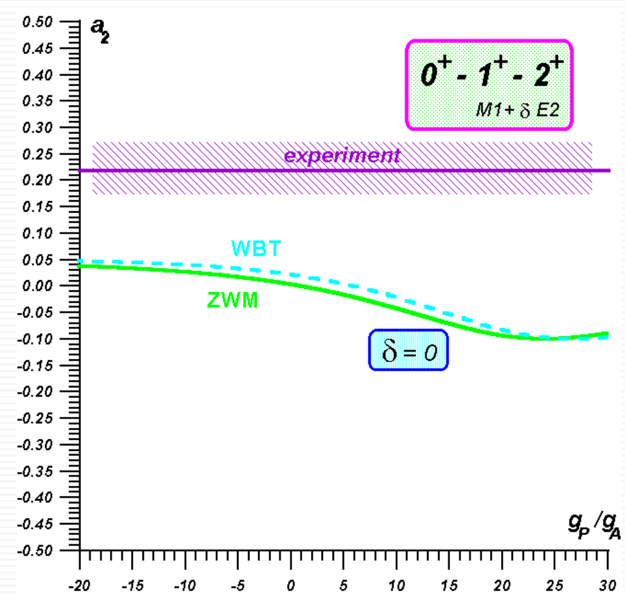

- Газовая мишень при давлении 1 атм.
- 4 HPGe детектора
- 400 часов измерений

Мишень: ^{48}Ti

Год исследования: 2002

Обогащение: 95.8%

Состав: TiO_2 порошок

Количество: 1.0 г

Полные скорости μ-захвата в ^{48}Ti

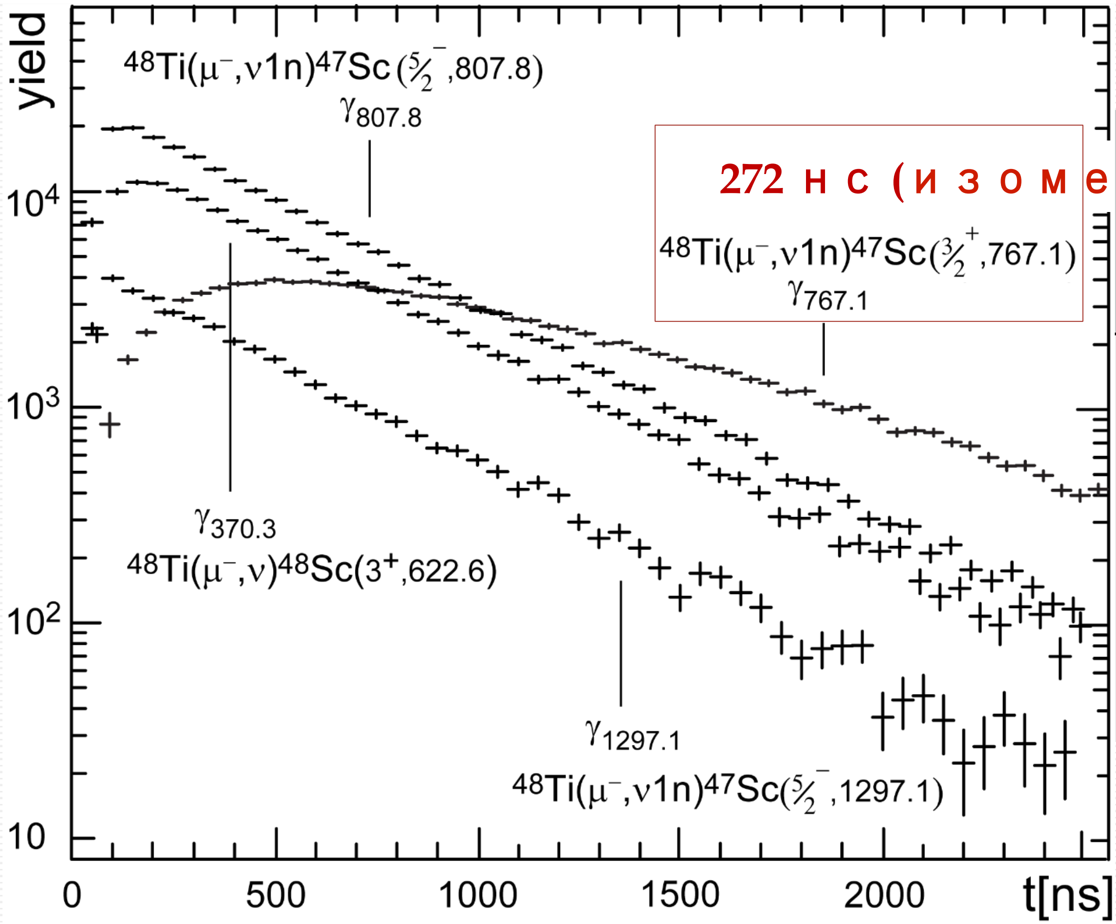

Мишень	Доч. ядро	E_i^{γ} [кэВ]	τ [нс]	$<\Lambda_{cap}>$ [10^6 c^{-1}]
^{48}Ti	^{48}Sc	370.3	363.8(26)	
	^{47}Sc	807.8	359.7(28)	
		1297.1	358.0(40)	
	^{47m}Sc	767.1	358(10) [+272 нс]	
			<361.1(24)>	2.323(15)

Парциальные вероятности μ-захвата ^{48}Sc

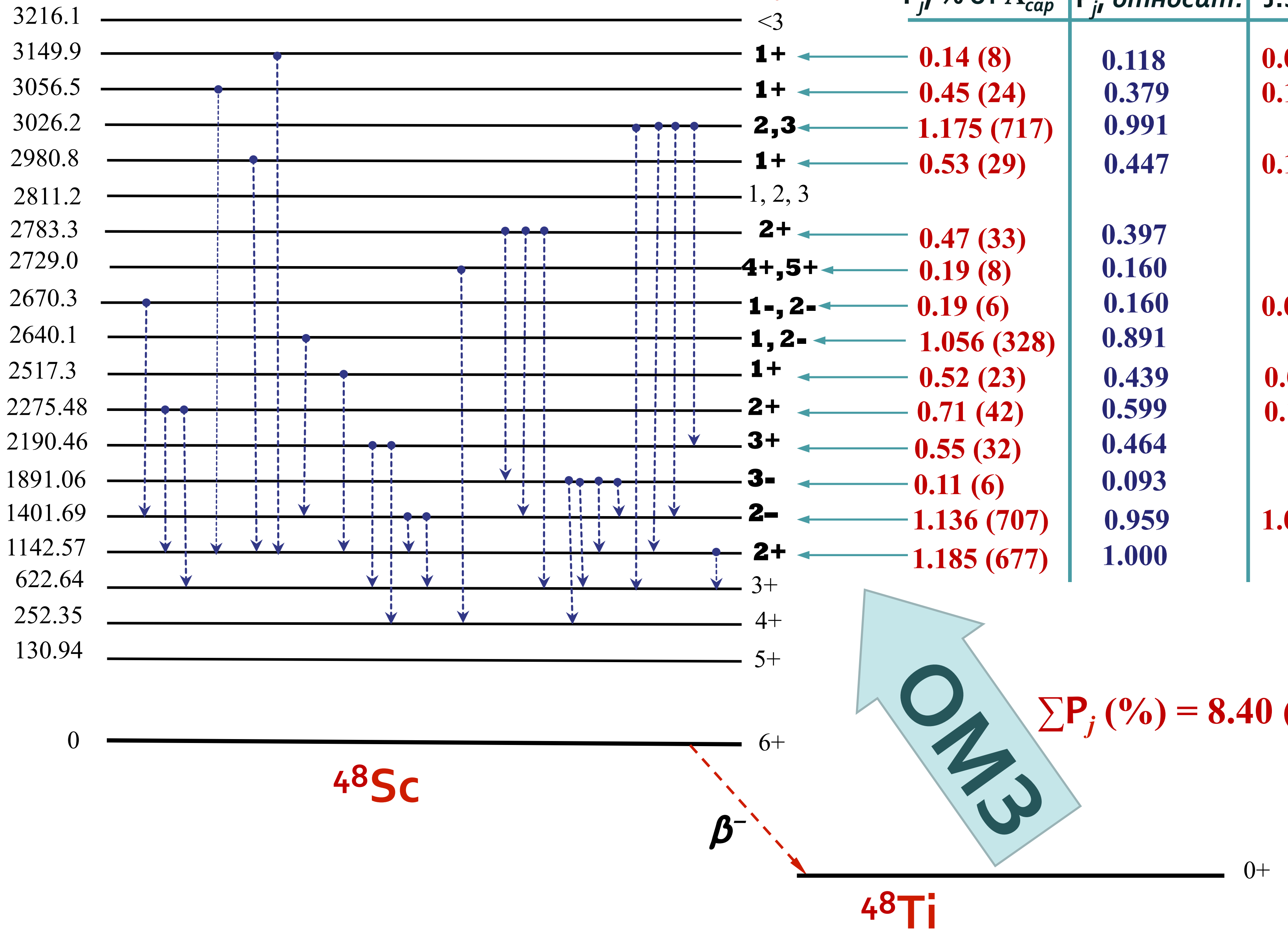

E, keV	J^{π}	P_j, % от Λ_{cap}	P_j, *относит.*	J.Suhonen et al.
3216.1	<3			
3149.9	1+	0.14 (8)	0.118	0.011
3056.5	1+	0.45 (24)	0.379	0.102
3026.2	2,3	1.175 (717)	0.991	
2980.8	1+	0.53 (29)	0.447	0.128
2811.2	1, 2, 3			
2783.3	2+	0.47 (33)	0.397	
2729.0	4+,5+	0.19 (8)	0.160	
2670.3	1-, 2-	0.19 (6)	0.160	0.080
2640.1	1, 2-	1.056 (328)	0.891	
2517.3	1+	0.52 (23)	0.439	0.050
2275.48	2+	0.71 (42)	0.599	0.195
2190.46	3+	0.55 (32)	0.464	
1891.06	3-	0.11 (6)	0.093	
1401.69	2-	1.136 (707)	0.959	1.000
1142.57	2+	1.185 (677)	1.000	
622.64	3+			
252.35	4+			
130.94	5+			
0	6+			

$\sum P_j (\%) = 8.40 (157)$

Мишени: ^{106}Cd, ^{nat}Cd

Год исследования: 2004

^{106}Cd

Обогащение: 63.0%

Состав: Cd (метал. фольга)

Количество: 5.0 г

^{nat}Cd

Состав: Cd (метал. фольга)

Количество: 5.0 г

Полные скорости μ-захвата в различных изотопах Cd

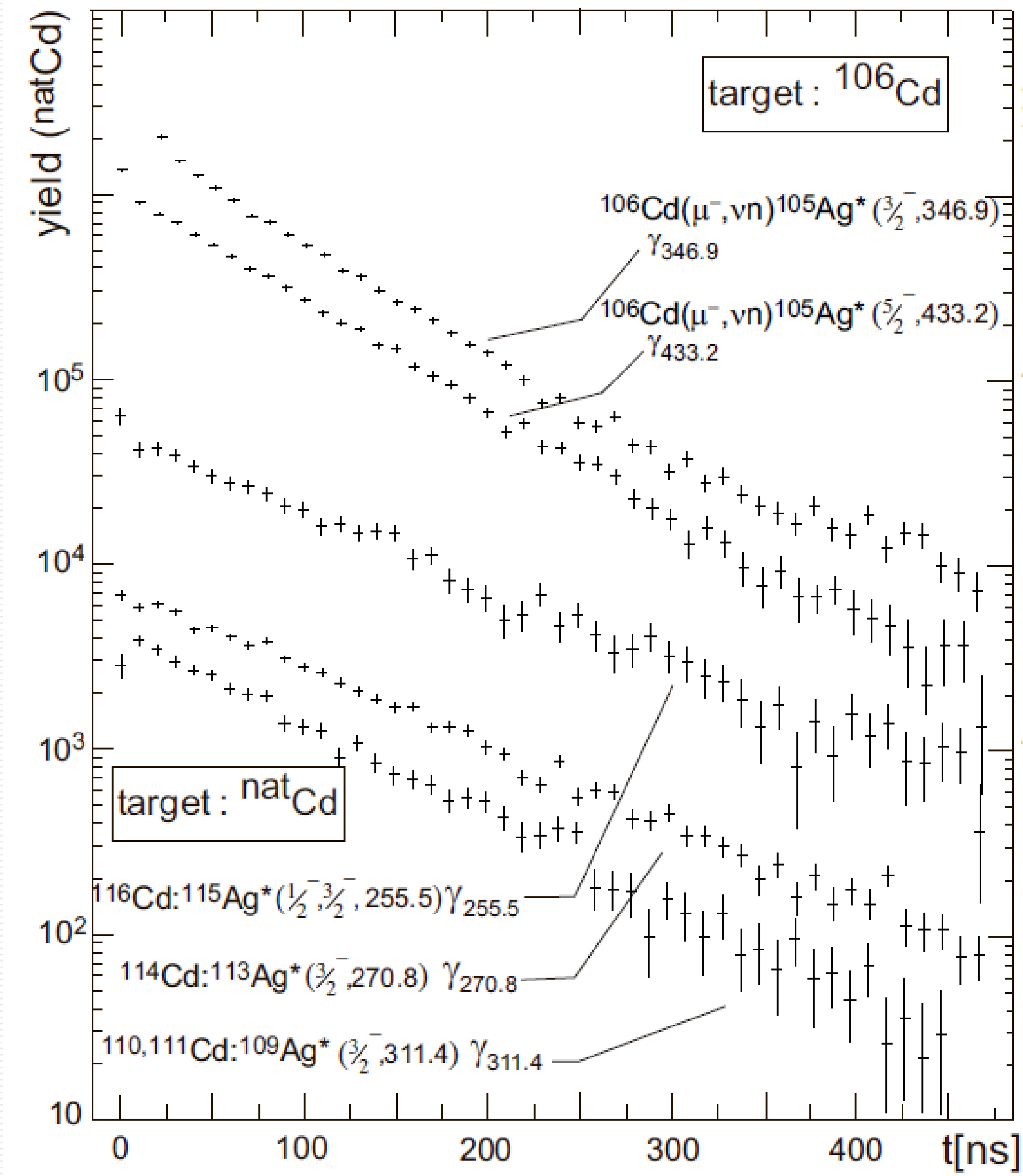

Мишень	Доч. ядро	E_i^{γ} [кэВ]	τ [нс]	$\langle\Lambda_{cap}\rangle$ [10^6 c^{-1}]
^{106}Cd	^{105}Ag	346.8	73.2(5)	
		433.2	72.4(8)	
			<72.97(36)>	13.28(7)
^{nat}Cd				
$^{(110,111)}$Cd	^{109}Ag	311.4	92.2(26)	10.43(31)
$^{(111,112)}$Cd	^{110}Ag	483.7	95.0(70)	10.11(75)
$^{(111,112)}$Cd	^{111}Ag	391.3	<99.45(5)>	9.600(5)
$^{(113,114)}$Cd	^{113}Ag	270.8	<102.07(15)>	9.380(14)
^{116}Cd	^{115}Ag	255.5	107.7(18)	8.86(15)

Парциальные вероятности μ-захвата

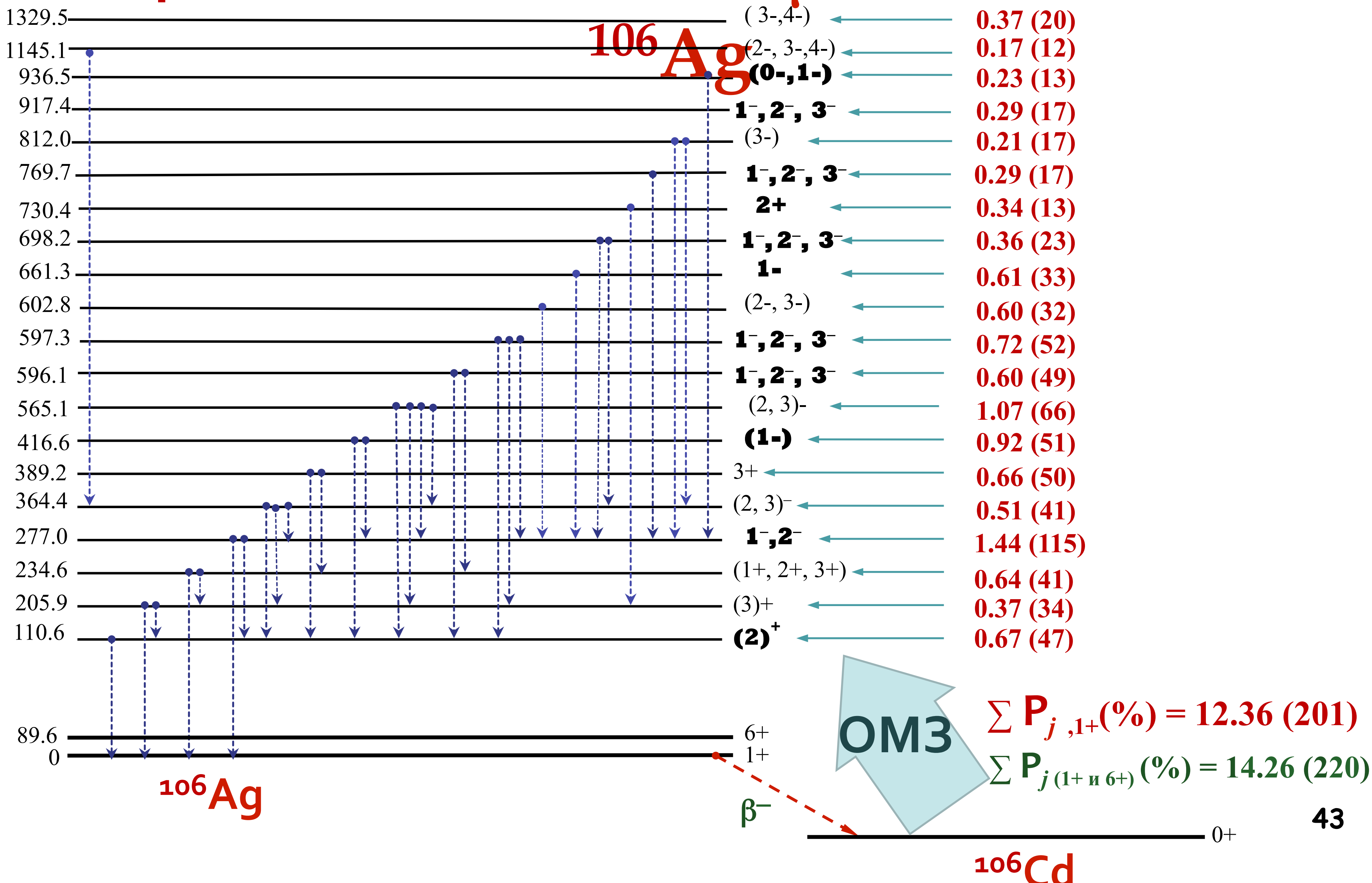

Мишени: ^{150}Sm, ^{nat}Sm

Год исследования: 2006

^{150}Sm

Обогащение: 92.6%

Состав: Sm_2O_3 (порошок)

Количество: 2.0 г

^{nat}Sm (тестовое измерение)

Состав: Sm_2O_3 (порошок)

Количество: 2.0 г

Полные скорости μ-захвата в ^{150}Sm

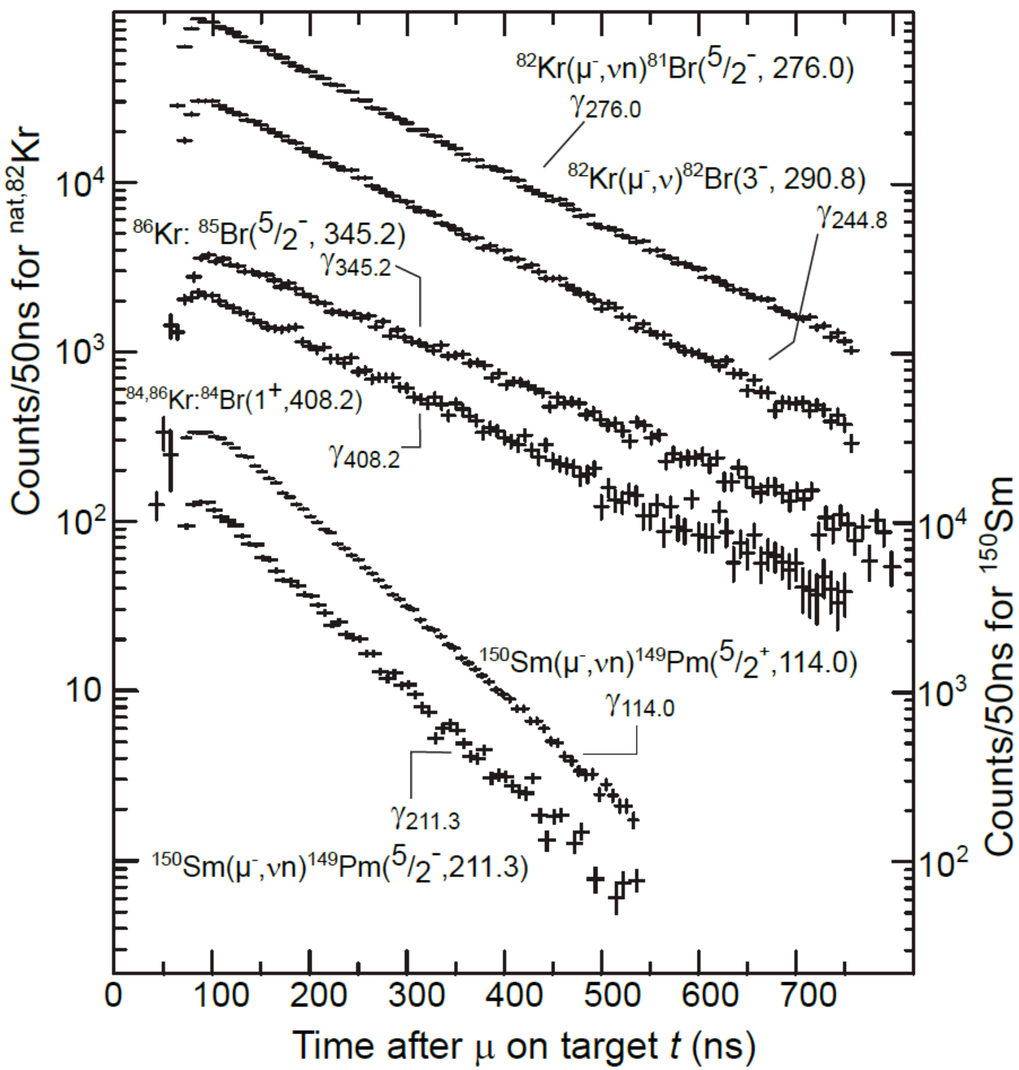

Мишень	Доч. ядро	E_i^{γ} [кэВ]	τ [нс]	<Λ_{cap}> [10^6 c^{-1}]
^{150}Sm	^{149}Pm	114.0	82.1(6)	
		211.2	81.8(9)	
	^{148}Pm	219.8	83.1(21)	
		233.0	81.7(21)	
			<82.3(5)>	11.75(7)

Анализ энергетических спектров, измеренных с ^{150}Sm

- Проведена идентификация μX-лучей (P) и γ-линий (D), получены парциальные интенсивности более 100 γ-переходов;
- Не было доступной информации о структуре возбужденных состояний ^{150}Pm (анализ данных продолжается);
- В U-спектрах идентифицировано семь изотопов/изомеров, определены выходы этих ядер в $(\mu^- + {}^{150}Sm)$ реакции.

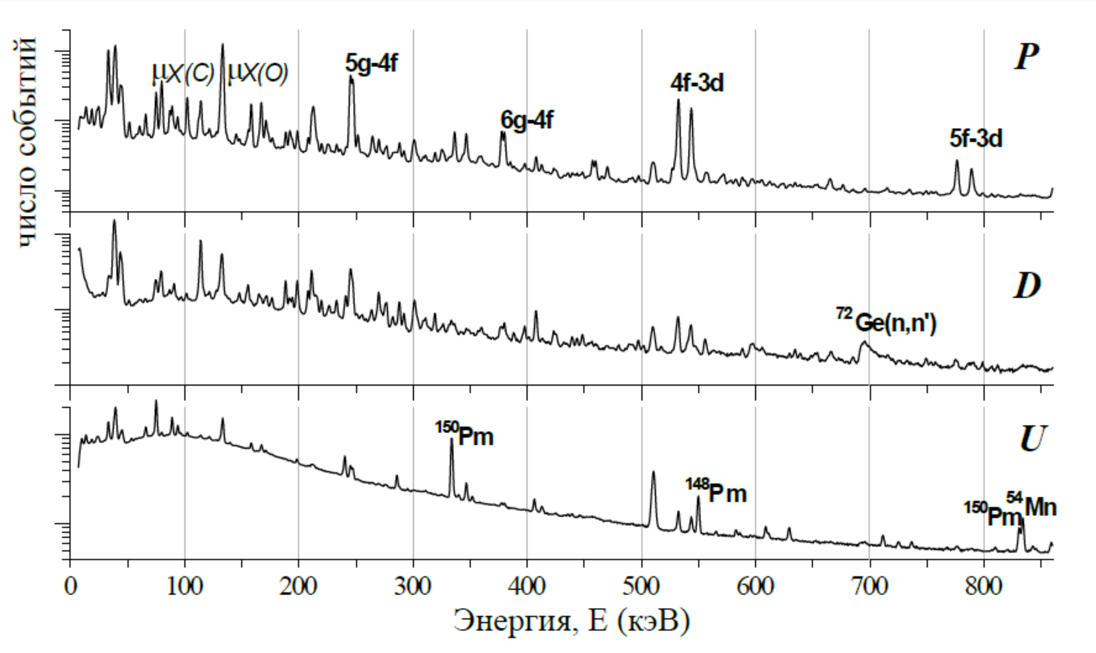

Изотоп	Вид распада	$T_{1/2}$	Λ_{cap} (xn yp) [10^6 c^{-1}]	P_{cap} [%]
^{150}Pm	β^-	2.68 ч	1.45(11)	12.3(9)
^{149m}Pm	IT	35 мкс	1.80(31)	15.3(26)
^{149}Pm	β^-	53.1 ч	2.93(60)	24.9(51)
^{148}Pm	β^-	5.37 д	0.77(26)	6.6(22)
^{148m}Pm	IT	41.3 д	0.10(2)	0.85(17)
^{148m}Pm	β^-	41.3 д	0.21(6)	1.79(51)
^{149}Nd	β^-	1.73 ч	0.78(35)	6.6(29)
^{148}Nd	стабильный		не измерен	
				∑=68.3(69)

Мишени: ^{82}Kr, ^{nat}Kr

Год исследования: 2006

<u>^{82}Kr</u>

Обогащение: 99.8%

Состав: Kr (газ)

Количество: 1.0 л (1 атм.)

<u>^{nat}Kr</u>

Состав: Kr (газ)

Количество: 1.0 л (1 атм.)

Полные скорости μ-захвата в различных изотопах Kr

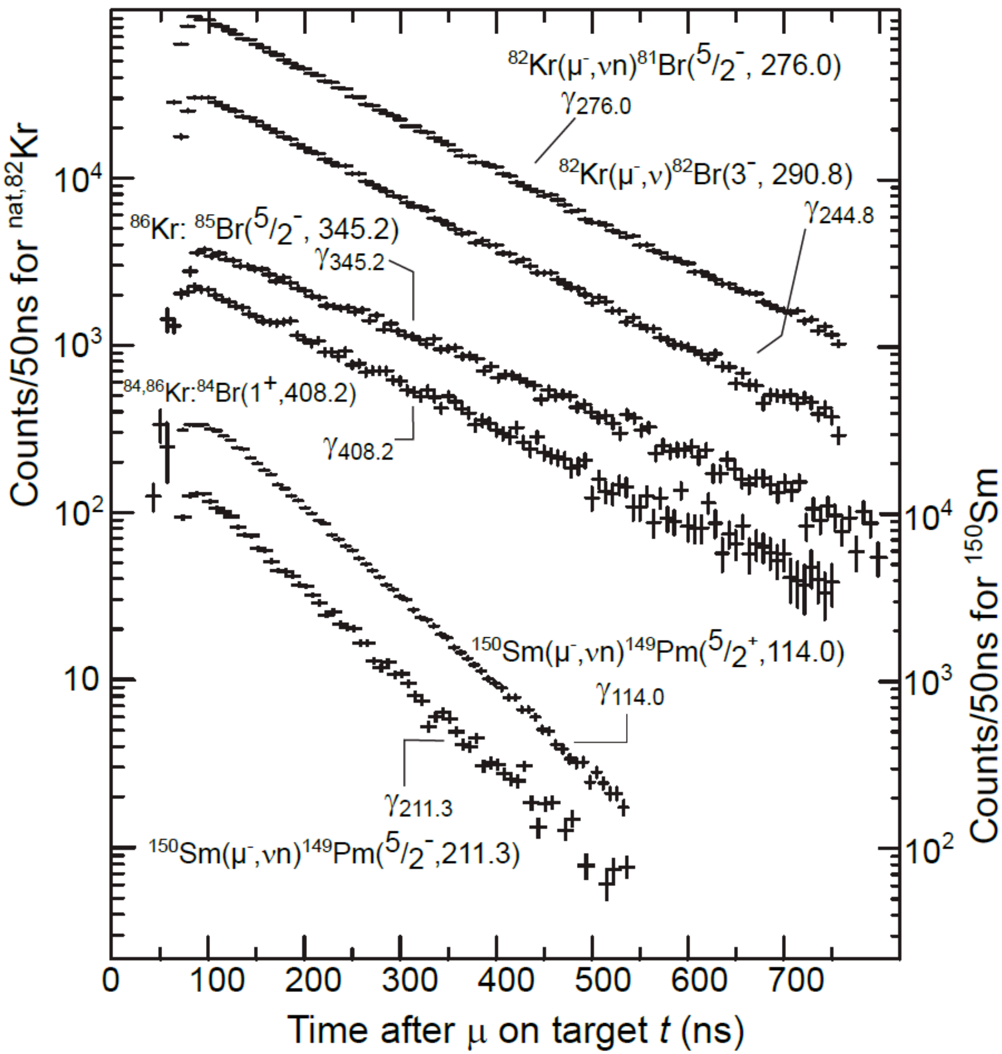

Мишень	Доч. ядро	E_i^{γ} [кэВ]	τ [нс]	$\langle\Lambda_{cap}\rangle$ [10^6 c^{-1}]
^{82}Kr	^{82}Br	244.8	142.9(6)	
	^{81}Br	276.0	142.6(3)	
			<142.68(37)>	6.576(17)
^{nat}Kr				
^{84}Kr	^{84}Br	408.2	160.1(27)	5.81(10)
^{86}Kr	^{85}Br	233.0	173.5(26)	5.33(8)

Оценка погрешности

Извлекаемое значение	Источник ошибки	Ошибка, %	Комментарии
ΔI_i^γ	площадь пика	1–25	зависит от интенсивности линии и фона
	эффективность детектора	5–20	возрастает в низком и высоком диапазонах энергий
	относительная интенсивность ‡	2–30	взяты из [48]
ΔY_j	сумма ошибок $\Delta I_{\text{in}}^\gamma$ и $\Delta I_{\text{out}}^\gamma$	22–43	зависит от полного количества заселяющих и разряжающих уровень γ-линий
ΔP_j	ΔY_j	22–43	
	$\Delta\lambda_{\text{tot}}$	0.06–0.6	зависит от примеси более тяжелого изотопа в обогащенной мишени
	$\Delta\lambda_{\text{cap}}$	0.06–0.6	зависит от примеси более тяжелого изотопа в обогащенной мишени

‡) использовалась только в случаях, когда извлечение абсолютной интенсивности γ-пика было сомнительным.